



HAL
open science

New material of *Incadelphys antiquus* (Pucadelphyda, Metatheria, Mammalia) from the early Palaeocene of Bolivia reveals phylogenetic affinities with enigmatic North and South American metatherians

Christian de Muizon, Sandrine Ladevèze

► **To cite this version:**

Christian de Muizon, Sandrine Ladevèze. New material of *Incadelphys antiquus* (Pucadelphyda, Metatheria, Mammalia) from the early Palaeocene of Bolivia reveals phylogenetic affinities with enigmatic North and South American metatherians. *Geodiversitas*, 2022, 44 (22), pp.609-643. 10.5252/geodiversitas2022v44a22 . hal-03888613

HAL Id: hal-03888613

<https://hal.science/hal-03888613>

Submitted on 7 Dec 2022

HAL is a multi-disciplinary open access archive for the deposit and dissemination of scientific research documents, whether they are published or not. The documents may come from teaching and research institutions in France or abroad, or from public or private research centers.

L'archive ouverte pluridisciplinaire **HAL**, est destinée au dépôt et à la diffusion de documents scientifiques de niveau recherche, publiés ou non, émanant des établissements d'enseignement et de recherche français ou étrangers, des laboratoires publics ou privés.

New material of *Incadelphys antiquus*
(Pucadelphyda, Metatheria, Mammalia)
from the early Palaeocene of Bolivia
reveals phylogenetic affinities with enigmatic
North and South American metatherians

Christian de MUIZON &
Sandrine LADEVÈZE



DIRECTEUR DE LA PUBLICATION / *PUBLICATION DIRECTOR* : Bruno David,
Président du Muséum national d'Histoire naturelle

RÉDACTEUR EN CHEF / *EDITOR-IN-CHIEF*: Didier Merle

ASSISTANT DE RÉDACTION / *ASSISTANT EDITOR*: Emmanuel Côté (geodiv@mnhn.fr)

MISE EN PAGE / *PAGE LAYOUT*: Emmanuel Côté

COMITÉ SCIENTIFIQUE / *SCIENTIFIC BOARD*:

Christine Argot (Muséum national d'Histoire naturelle, Paris)
Beatrix Azanza (Museo Nacional de Ciencias Naturales, Madrid)
Raymond L. Bernor (Howard University, Washington DC)
Henning Blom (Uppsala University)
Jean Broutin (Sorbonne Université, Paris, retraité)
Gaël Clément (Muséum national d'Histoire naturelle, Paris)
Ted Daeschler (Academy of Natural Sciences, Philadelphie)
Bruno David (Muséum national d'Histoire naturelle, Paris)
Gregory D. Edgecombe (The Natural History Museum, Londres)
Ursula Göhlich (Natural History Museum Vienna)
Jin Meng (American Museum of Natural History, New York)
Brigitte Meyer-Berthaud (CIRAD, Montpellier)
Zhu Min (Chinese Academy of Sciences, Pékin)
Isabelle Rouget (Muséum national d'Histoire naturelle, Paris)
Sevket Sen (Muséum national d'Histoire naturelle, Paris, retraité)
Stanislav Štamberg (Museum of Eastern Bohemia, Hradec Králové)
Paul Taylor (The Natural History Museum, Londres, retraité)

COUVERTURE / *COVER*:

Réalisée à partir des Figures de l'article/*Made from the Figures of the article.*

Geodiversitas est indexé dans / *Geodiversitas is indexed in*:

- Science Citation Index Expanded (SciSearch®)
- ISI Alerting Services®
- Current Contents® / Physical, Chemical, and Earth Sciences®
- Scopus®

Geodiversitas est distribué en version électronique par / *Geodiversitas is distributed electronically by*:

- BioOne® (<http://www.bioone.org>)

Les articles ainsi que les nouveautés nomenclaturales publiés dans *Geodiversitas* sont référencés par /
Articles and nomenclatural novelties published in Geodiversitas are referenced by:

- ZooBank® (<http://zoobank.org>)

Geodiversitas est une revue en flux continu publiée par les Publications scientifiques du Muséum, Paris
Geodiversitas is a fast track journal published by the Museum Science Press, Paris

Les Publications scientifiques du Muséum publient aussi / *The Museum Science Press also publish: Adansonia, Zoosystema, Anthropozoologica, European Journal of Taxonomy, Naturae, Cryptogamie* sous-sections *Algologie, Bryologie, Mycologie, Comptes Rendus Palevol*

Diffusion – Publications scientifiques Muséum national d'Histoire naturelle
CP 41 – 57 rue Cuvier F-75231 Paris cedex 05 (France)
Tél.: 33 (0)1 40 79 48 05 / Fax: 33 (0)1 40 79 38 40
diff.pub@mnhn.fr / <http://sciencepress.mnhn.fr>

© Publications scientifiques du Muséum national d'Histoire naturelle, Paris, 2022
ISSN (imprimé / *print*): 1280-9659/ ISSN (électronique / *electronic*): 1638-9395

New material of *Incadelphys antiquus* (Pucadelphyda, Metatheria, Mammalia) from the early Palaeocene of Bolivia reveals phylogenetic affinities with enigmatic North and South American metatherians

Christian de MUIZON
Sandrine LADEVÈZE

CR2P (CNRS, MNHN, UPMC, Sorbonne Université), Muséum national d'Histoire naturelle, case postale 38, 57 rue Cuvier, F-75231 Paris cedex 05 (France)
muizon@mnhn.fr

Submitted on 1 July 2021 | accepted on 7 October 2021 | published on 30 June 2022

urn:lsid:zoobank.org:pub:B8864E92-2EC0-4E0A-97F1-BFAE94DC24D8

Muizon C. de & Ladevèze S. 2022. — New material of *Incadelphys antiquus* (Pucadelphyda, Metatheria, Mammalia) from the early Palaeocene of Bolivia reveals phylogenetic affinities with enigmatic North and South American metatherians. *Geodiversitas* 44 (22): 609-643. <https://doi.org/10.5252/geodiversitas2022v44a22>. <http://geodiversitas.com/44/22>

ABSTRACT

The present paper describes a partial skull referred to *Incadelphys antiquus*, from the early Palaeocene of Tiupampa (Bolivia). The specimen includes the anterior part of the skull with maxillae, premaxillae, nasals, lacrimals, anterior part of frontals and jugal, and both dentaries. Most of the teeth are preserved except some incisors. Some of the major characteristics of *Incadelphys* are the elongation and slenderness of the rostrum as compared to other Tiupampa taxa and the narrowness and blade-like morphology of the premolars. The new specimen is compared to the other Tiupampian pucadelphydians, especially, pucadelphyids, but also sparassodonts. Comparisons with *Marmosopsis juradoi*, from the early Eocene of Itaboraí and with *Aenigmadelphys archeri* from the latest Campanian of North America is also meaningful. Among others, the three genera share a strong distolabial extension of their metastylar area of the M1, which has not been observed, to a such extent, in other American metatherians. A phylogenetic parsimony analysis has been performed with exclusion some poorly known taxa, such as *Jaskhadelphys minutus* (two upper molars only), from Tiupampa or *Kiruwamaq chisu* (one M₃ only) from the late Eocene of Peru. The taxa included in our analysis are at least known from all upper and lower molars. The result of our analysis with unweighted characters retrieved the inclusion of *Incadelphys*, *Marmosopsis*, *Szalinia* and *Aenigmadelphys* in the clade Pucadelphyda, which also includes the Pucadelphyidae and the Sparassodonta. An analysis with downweighted homoplastic characters (with Goloboff K=3) resulted in a monophyletic grouping of *Szalinia*, *Aenigmadelphys*, *Marmosopsis*, and *Incadelphys* in an unnamed clade designated with the working term SAMI (after the initial of these four genera). This result, which we favor, is the first hypothesis which suggests a close relationship between the early Palaeocene - early Eocene, Tiupampa -Itaboraí pucadelphydians and a Late Cretaceous North American taxon, *Aenigmadelphys*, which is included within the Pucadelphyda.

KEY WORDS

Metatheria,
Pucadelphyda,
Marsupialia,
early Palaeocene,
Palaeogene,
Tiupampa,
Bolivia,
cranial anatomy,
phylogeny,
new superfamily.

RÉSUMÉ

Le nouveau matériel d'Incadelphys antiquus (Pucadelphyda, Metatheria, Mammalia) provenant du Paléocène inférieur de Bolivie révèle des affinités phylogénétiques avec des métathériens énigmatiques d'Amérique du Nord et du Sud.

Le présent article décrit un crâne partiel rapporté à *Incadelphys antiquus*, du Paléocène inférieur de Tiupampa (Bolivie). Ce spécimen comprend la partie antérieure du crâne avec les maxillaires, les prémaxillaires, les nasaux les lacrimaux, la partie antérieure des frontaux et des jugaux et les deux dentaires. La plupart des dents sont préservées à l'exclusion de quelques incisives. Les principales caractéristiques d'*Incadelphys* sont l'allongement et la gracilité du rostre, comparés aux autres taxons de Tiupampa et l'étréoussse et la morphologie en lame de ses prémolaires. Le nouveau spécimen est comparé aux autres pucadelphidiens de Tiupampa, particulièrement les pucadelphidés mais aussi les sparassodontes. Une comparaison avec *Marmosopsis juradoi* de l'Éocène inférieur d'Itaboraí et avec *Aenigmadelphys archeri* du Campanien terminal d'Amérique du Nord est également riche en enseignements. Entre autres, les trois genres possèdent en commun une forte extension disto-labiale de la région métastylaire de leur M1, qui n'a été observée à un tel degré chez aucun autre métathérien américain. Une analyse phylogénétique de parcimonie a été réalisée en excluant les taxons connus par du matériel trop fragmentaire tels que *Jaskhadelphys minutus*, (deux molaires supérieures seulement) de Tiupampa et *Kiruwamaq chisu* (une M?3 seulement) de l'Éocène supérieur du Pérou. Les taxons inclus dans notre analyse sont connus au moins par toutes leurs molaires supérieures et inférieures. Le résultat de notre analyse sans pondération des caractères a inclus *Incadelphys*, *Marmosopsis*, *Szalinia* et *Aenigmadelphys* dans le clade Pucadelphyda, qui inclut aussi les Pucadelphyidae et les Sparassodonta. Une analyse avec pondération implicite (avec une valeur K = 3 pour la constante de Goloboff) a produit un regroupement monophylétique de *Szalinia*, *Aenigmadelphys*, *Marmosopsis* et *Incadelphys* en un clade non nommé, désigné sous le terme de travail SAMI (d'après les initiales de ces quatre genres). Ce résultat, qui a notre préférence, est la première hypothèse qui propose une relation étroite entre les pucadelphidés du Paléocène inférieur-Éocène inférieur de Tiupampa-Itaboraí et un taxon du Crétacé supérieur d'Amérique du Nord, *Aenigmadelphys*, qui est ici inclus dans les Pucadelphyda.

MOTS CLÉS
Metatheria,
Pucadelphyda,
Marsupialia,
Paléocène inférieur,
Paléogène,
Tiupampa,
Bolivie,
anatomie crânienne,
phylogénie,
superfamille nouvelle.

INTRODUCTION

The earliest metatherian fauna of South America is from the early Palaeocene of Tiupampa (Cochabamba Department, Bolivia) (see Muizon & Ladevèze 2020 for a review of the age of Tiupampa mammal bearing beds). It is already quite diverse since it includes at least 12 species and genera. Several metatherian taxa from Tiupampa are referred to taxonomic groups well diversified in the later Cenozoic of South America. They are *Roberthoffstetteria* (Polydolopimorphia), *Mayulestes* and *Allqokirus* (Sparassodonta), *Khasia* (Microbiotheria, but see Goin *et al.* 2016 and Muizon & Ladevèze 2020), *Peradectes* cf. *P. austrinum* (Peradectia). Other taxa have been included in a new family (Pucadelphyidae, Muizon 1998) characteristic of the Tiupampa fauna. They are *Pucadelphys*, *Andinodelphys* and *Mizquedelphys*. Recently Muizon & Ladevèze (2020) have also included in the Pucadelphyidae the genus *Itaboraidelphys* from the early Eocene of Itaboraí (Brazil), which has been retrieved as sister taxon of *Pucadelphys* and *Andinodelphys*. Furthermore, four recently identified sub-complete and partial skulls of *Mizquedelphys* are currently under study by the authors. The other metatherian taxa of Tiupampa are still of uncertain taxonomic affinities because their remains are essentially dental and not as complete as those of the other taxa. These taxa (*Incadelphys*, *Tiulordia*, and *Szalinia*) are not easily related to other well-known taxa from North or South America. Because of this difficulty, they have been frequently regarded as “Ameridelphia”

incertae sedis and have not been included in a specific family (Goin *et al.* 2016; Muizon *et al.* 2018). Finally, *Jaskhadelphys minutus*, which is known from a single maxillary fragment with M2-M3, has been regarded by Marshall & Muizon (1988) as closely related to *Minusculodelphis minimus* from the early Eocene of Itaboraí (Brazil). Muizon (1992) created the new family, Jaskhadelphyidae, in which Goin *et al.* (2016) included *Minusculodelphis*. Oliveira *et al.* (2016) revised the taxonomy and affinities of *Minusculodelphis* and referred to this taxon, several upper and lower molars of a new species (*M. modicum*), which seems to reinforce the comparison and conclusions of Marshall & Muizon (1988). Oliveira *et al.* (2016) also included in Jaskhadelphyidae, *Kiruwamaq chisu* from the late Eocene of Peru, a taxon known from a single M?3 only (Goin & Candela 2004). Although the monophyly of the family retrieved by Oliveira *et al.* (2016) appears convincing, the taxonomy and affinities of Jaskhadelphyidae remains uncertain at a higher taxonomic level (McKenna & Bell 1997; Goin *et al.* 2016; Muizon *et al.* 2018).

In this context, we describe here a partial skull referred to *Incadelphys minutus* and some isolated dental remains, discovered after the description of the holotype by Marshall & Muizon (1988). The partial skull includes almost complete upper and lower dentitions and the anterior half of the skull, and will be described in order to analyze its relationships with other Tiupampa and Itaboraí metatherians, as well as some North American taxa such as *Aenigmadelphys* from the late Campanian of Utah.

MATERIAL AND METHODS

SPECIMENS DESCRIPTION AND COMPARISON

Incadelphys antiquus was named on the basis of the partial maxillaries and mandibles of a sub-adult specimen (YFPB Pal 6151). The discovery of a partial skull of the same species with almost complete dentition, and several other isolated specimens (teeth or jaw fragment) allows a more thorough knowledge of this taxon. The new specimens will be compared to other Tiupampan taxa such as *Mizquedelphys* and *Szalinia*, as well as with another South American taxon from the early Eocene of Itaboraí, *Marmosopsis juradoi*, which has been regarded as remarkably similar to *Incadelphys* by Marshall & Muizon (1988). The specimens described below will also be compared to the enigmatic North American metatherian from the latest Campanian of North America, *Aenigmadelphys archeri*, with which the *Incadelphys* shows great similarities.

PHYLOGENETIC ANALYSIS

The phylogenetic analysis performed here used the data matrix of Ladevèze *et al.* (2020) to which we added the taxa employed in the comparison, to which *Incadelphys* compares most favorably: *Marmosopsis*, *Szalinia*, and *Aenigmadelphys*. We also added *Itaboraidelphys*, which has been retrieved by Muizon & Ladevèze (2020) as a sister taxon of *Pucadelphys* and *Andinodelphys*. However, we have removed *Patene*, which is known essentially from dental remains and which is not highly relevant to the present study; we have only retained three sparassodont taxa known from excellent cranial and postcranial material. We have not included *Jaskhadelphys* because we judge its material too scarce, being known from a single specimen with two upper molars only. *Tiulordia* has not been included either in our analysis because the recent discovery of more complete dental material of this taxon requires its revision, which is beyond the focus of the present study.

Following Muizon *et al.* (2018: 422–423; 2020) we have referred the Type II petrosal from Itaboraí (Ladevèze 2004; Ladevèze & Muizon 2010) to the dental remains of *Itaboraidelphys camposi*, an interpretation, which is established on the basis of a morphometric comparison with the remarkably preserved skulls of *Andinodelphys* from Tiupampa. This referral is also based on the phylogenetical relationships of Type II Petrosal, which is retrieved as sister group to the *Pucadelphys-Andinodelphys* clade (Ladevèze & Muizon 2010). In contrast, we have not scored petrosal characters for *Marmosopsis* because two taxa (*M. juradoi* and *Gaylordia doeloi*) could be referred on the basis of morphometry to three petrosal types (III, V, and VII). Furthermore, none of these three petrosals have been retrieved as closely related to *Marmosopsis* in the phylogenetic analysis performed by Ladevèze & Muizon (2010), which casts doubt on a secure referral of one of the three petrosal types to dental remains of *Marmosopsis juradoi*.

The character list of Ladevèze *et al.* (2020) has been increased with one new character: the posterolabial exten-

sion of the metastylar angle of M1 as brought to light in the description of the molars below. The new character (36) is described below:

Character 36: Extreme posterolabial extension and narrowing of metastylar angle of M1, 0) angle between the stylar cusps D-E axis and the postmetacrista > 40°; 1) angle between the stylar cusps D-E axis and the postmetacrista = or < 40°. Furthermore, a third character state has been added to character 18: state 2, premolars blade-like (i.e. the width of premolar is less than 40% the length). Because these changes are minor, the character list of Ladevèze *et al.* (2020) is not reproduced here. However, a comment on the scoring of character 37 for *Marmosopsis* is discussed in Appendix 1.

Our data set comprises a total of 287 osteological characters (79 dental, 11 mandibular, 99 cranial, 98 post-cranial), examined in three outgroup and 29 ingroup taxa (fossil and extant metatherians). The outgroup taxa include three fossil eutherians, the sister group to Metatheria. The former includes *Prokennalestes* from the Early Cretaceous of Mongolia, which is known from upper and lower postcanine teeth, dentaries, and one petrosal (Kielan-Jaworowska & Dashzeveg 1989; Sigogneau-Russell *et al.* 1992; Wible *et al.* 2001). Furthermore, in a recent monograph Lopatin & Averianov (2017) described and illustrated a remarkably abundant new material of *Prokennalestes* including several hundred upper and lower jaws and teeth from the locality of Khovoor in the Gobi Desert of Mongolia. Other outgroup taxa are *Maelestes*, represented by the skull, mandible, anterior vertebrae, and partial left forelimb (Wible *et al.* 2009), and *Asioryctes*, represented by several complete skulls and skeletons from the Late Cretaceous of Mongolia (Kielan-Jaworowska 1977, 1981).

The taxon/character states matrix was analyzed using heuristic parsimony searches implemented by PAUP* (Swofford 2002). Each heuristic parsimony search employed 100 replicates of random taxon addition with TBR branch swapping, saving up to 10 trees. Two analyses were performed, one with unweighted characters, and the other with implied weighting with the Goloboff constant value = 3. The use of higher Goloboff constant value (as recommended by Goloboff *et al.* 2017) retrieved consensus trees almost identical to the strict consensus and did not downweight homoplastic characters, which justifies the selection of a low value of the Goloboff constant (3) in the present study. The resulting phylogenetic trees with morphological character state optimizations were generated by PAUP* (Swofford 2002) and Winclada v.1.00.08 (Nixon 2008). Polymorphic taxa were coded with multiple character state entries. Most multistate characters were treated as unordered, but 13 of them were considered as additive because previous studies have assumed they are morphoclines or because we suspected them to be (Rougier *et al.* 1998; Wible *et al.* 2001; Ladevèze & Muizon 2007). Branch support was assessed by calculating the Bremer index (Bremer 1988) with PAUP* (Swofford 2002) (heuristic searches with 100 replications, saving up to 10 trees, TBR branch swapping).

TERMINOLOGY, MEASUREMENTS, TAXON LIST AND MATERIAL
Anatomical terminology for the skull essentially follows Wible (2003, 2008, 2011) and Wible & Spaulding (2013) unless specified. Dental terminology is presented on Fig. 1. Lower incisor homology follows Hershkovitz (1982, 1995). Dental measurements follow Gheerbrant (1992: fig. 4). Internal edge of the teeth (i.e. on the side of the mouth and tongue) will be designated as lingual and external edge (i.e. on the side of the vestibulum, lips or cheeks), will be designated as labial, although the last molars are generally bordered by the cheek rather than the lip.

Appendix 2 provides a list of the taxa and material available to us (original specimens with catalogue numbers, casts, photos, CT data, references). The list of generic and specific taxa cited in the text with authorship and date of publication is given in Appendix 3.

INSTITUTIONAL ABBREVIATIONS

AMNH	American Museum of Natural History, New York, United States;
BMNH	Beijing Museum of Natural History;
DGM	Divisão de Geologia e Mineralogia do Departamento Nacional da Produção Mineral, Rio de Janeiro, Brazil;
FMNH	Field Museum of Natural History, Chicago, Illinois, United States;
IEEUACG	Instituto de Ecología y Evolución, Universidad Austral de Chile, Valdivia, Chile;
MACN	Museo Argentino de Ciencias Naturales “Bernardino Rivadavia”, Buenos Aires, Argentina;
MB.Ma	Museum für Naturkunde, Berlin, Germany;
MHNC	Museo de Historia Natural “Alcide d’Orbigny”, Cochabamba, Bolivia;
MNHN	Muséum national d’Histoire naturelle, Paris, France;
MNRJ	Museu Nacional e Universidade Federal do Rio de Janeiro, Rio de Janeiro, Brazil;
NDGS	North Dakota Geological Survey, State Fossil Collection at the North Dakota Heritage Center State Museum, Bismarck, North Dakota, United States;
OMNH	Oklahoma Museum of Natural History, Norman, Oklahoma, United States;
PIMUZ	Paläontologisches Institute und Museum Zürich, Switzerland;
PIN	Paleontological Institute of the Russian Academy of Sciences;
PSS-MAE	Paleontological and stratigraphy Section (Geological Institute), Mongolian Academy of Sciences, Ulaan Baatar, Mongolia;
RH	Robert Hoffstetter collection of Recent vertebrates, in the MNHN, Muséum national d’Histoire naturelle, Paris, France;
SC	Sierra College Natural History Museum, Rocklin, California, United States;
SMF	Senckenberg, Museum of Natural History, Frankfurt, Germany;
SMP-SMU	Shuler Museum of Paleontology, Southern Methodist University, Dallas, United States;
STM	Tianyu Museum of Nature, Linyi, Shandong Province, China;
UCMP	Museum of Paleontology, University of California, Berkeley, United States;
UMC	Palaeontological collections of the Université Montpellier 2, France;
USNM	United States National Museum, Smithsonian Institution, Washington, DC, United States;
UWBM	University of Washington, Burke Museum of natural history and Culture, Seattle, Washington, United States;

YPFB	Yacimientos Petrolíferos Fiscales de Bolivia;
YPM-PU	Princeton University collection housed in the Yale Peabody Museum, Yale University, New Haven, Connecticut, United States;
ZPAL	Paleontological Institute of the Polish Academy of Sciences, Warsaw, Poland.

SUPPLEMENTARY DATA

Supplementary data are available at the following address:
https://doi.org/10.5852/geodiversitas2022v44a22_s1

PARSIMONY ANALYSIS FILES

File 1: NEXUS file of the data matrix.

SYSTEMATIC PALAEOLOGY

Infraclass METATHERIA Huxley, 1880
Superorder PUCADELPHYDA
Muizon, Ladevèze, Selva, Vignaud, Goussard, 2018
Order indet.

Superfamily PUCADELPHYOIDEA n. superfam.

NOTE

The superfamily Pucadelphyoidea n. superfam. includes two clades, the family Pucadelphyidae and an unnamed clade defined below. The Pucadelphyidae include the following genera: *Pucadelphys* Marshall & Muizon, 1988; *Andinodelphys* Marshall & Muizon, 1988; *Mizquedelphys* Marshall & Muizon, 1988, *Itaboraïdelphys* Marshall & Muizon, 1984.

The unnamed clade includes, in addition to *Incadelphys* Marshall & Muizon, 1988 the following genera: *Aenigmadelphys* Cifelli & Johanson, 1994, *Marmosopsis* Paula Couto, 1962, and *Szalinia* Muizon & Cifelli, 2001. As discussed in the phylogeny section below, we favor the topology resulting from the analysis with implied weighting of characters, which retrieved the four genera in a clade. However, we are reluctant to formally name this clade because we consider that *Jaskhadelphys* should be included in the taxon list (which we did not) but with substantial new and more complete specimens than the single maxillary fragment with M2-M3 known so far. If *Jaskhadelphys* was to be included in this clade (what is so far highly uncertain), then the resulting clade should be the family Jaskhadelphyidae (Muizon 1992).

Family unnamed

Genus *Incadelphys* Marshall & Muizon, 1988

DIAGNOSIS. — Because the genus is monospecific, its diagnosis is that of the type species.

TYPE SPECIES. — *Incadelphys antiquus* Marshall & Muizon, 1988 by original designation.

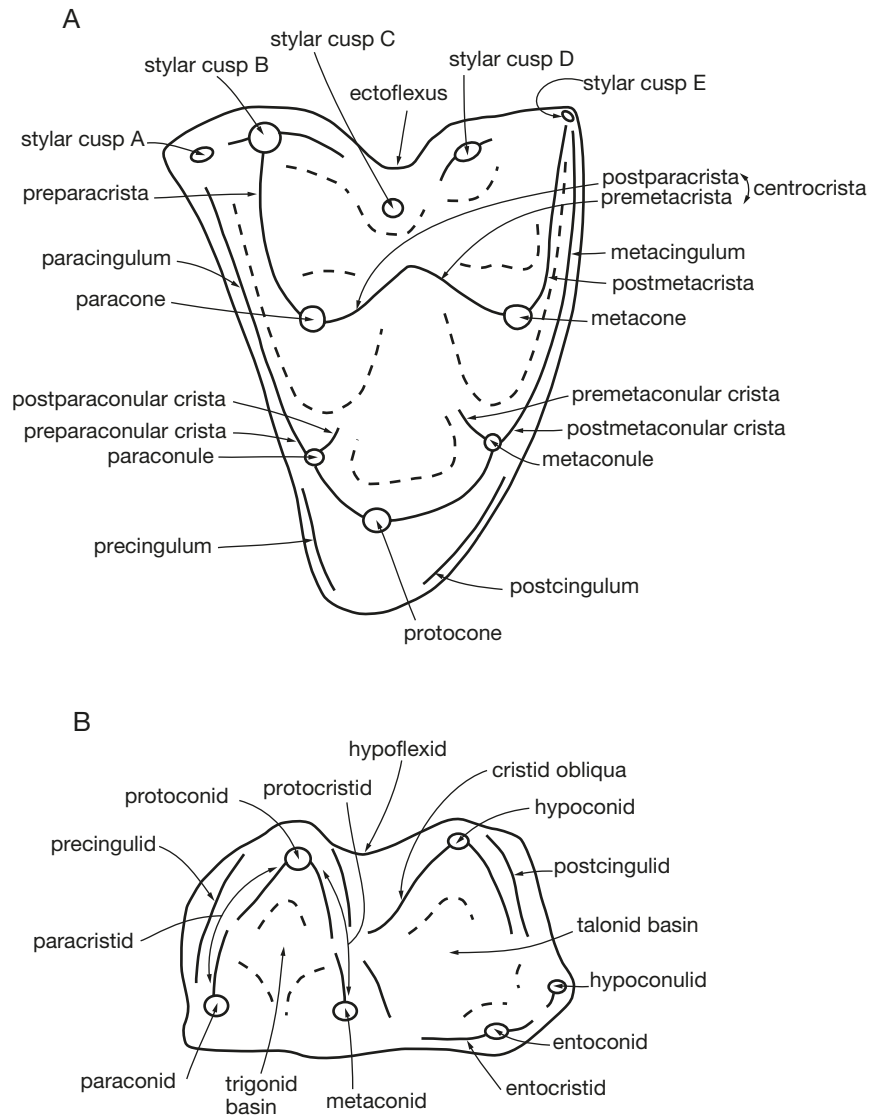


Fig. 1. — Dental terminology (redrawn and modified from Davis 2007).

Incadelphys antiquus Marshall & Muizon, 1988

HOLOTYPE. — YPFB Pal 6151, partial upper and lower jaws of the same juvenile specimen including the left maxilla with base of P1, P2, dP3, unerupted P3, M1-M3 (M3 erupting and missing tip of protocone); the right maxilla with dP3 unerupted P3, M1-M3 (M3 erupting); the right mandibular ramus with p1, p2, dp3, unerupted p3; m1-2, talonid of m3, unerupted m4; the left mandibular ramus with talonid of dp3, m1-2, m3 broken, m4 unerupted (Fig. 2)

EMENDED DIAGNOSIS. — Dental formula I5/i4, C/c, P3/p3; M4/m4; skull slightly smaller than *Pucadelphys* but distinctly larger than *Szalinia*; approaching the size of the extant didelphid *Thylamys*, proportions of the rostrum approaching those of *Pucadelphys* with the apex more slender; palatal vacuities absent.

Incadelphys antiquus differs from Pucadelphyidae in the following features: occurrence of a distinct lacrimal-nasal contact; extremely narrow and blade-like upper premolars, with weaker labial and lingual posterocingula (in pucadelphyids upper premolars are wider with thick labial and lingual posterocingula); upper molar smaller and more gracile; M1 strongly asymmetrical; distolabial angle of

M1 conspicuously extended distolingually with angle between labial edge of tooth and postmetacrista varying from 34° to 37° (in pucadelphyids the angle vary from 49° to 62°; mean = 51.4°); protocone mesiodistally shorter; mesiodistal constriction (i.e. shortening) at lingual base of para-metacone more pronounced, especially on M3, (in pucadelphyids constriction is weak to absent); posterolingual inflation of protocone absent or faint (in pucadelphyids posterolingual inflation present); centrocrista weakly V-shaped (in pucadelphyids V-shaped centrocrista is generally conspicuous); anterior styler shelf on M1 narrower; styler cusp C absent on M3, absent or small on M1-M2 (in pucadelphyids styler cusp C is generally present in M1-M3); when present, styler cusp C much smaller than B and D (in pucadelphyids styler cusp C is generally subequal to slightly smaller than D); distolabial angle of M1 extending distolabially to a greater extent, with angle between postmetacrista and lingual edge of the tooth smaller; ectoflexus totally absent on M1 (present in pucadelphyids) and shallower on M2-M3 (deep in pucadelphyids); ventral edge of dentary less convex; coronoid process distinctly narrower at apex and not recurved posteriorly (in other words posterior edge of process straight) (in pucadelphyids apex of coronoid process is strongly recurved posteriorly); retromolar space longer (almost as long as m4)

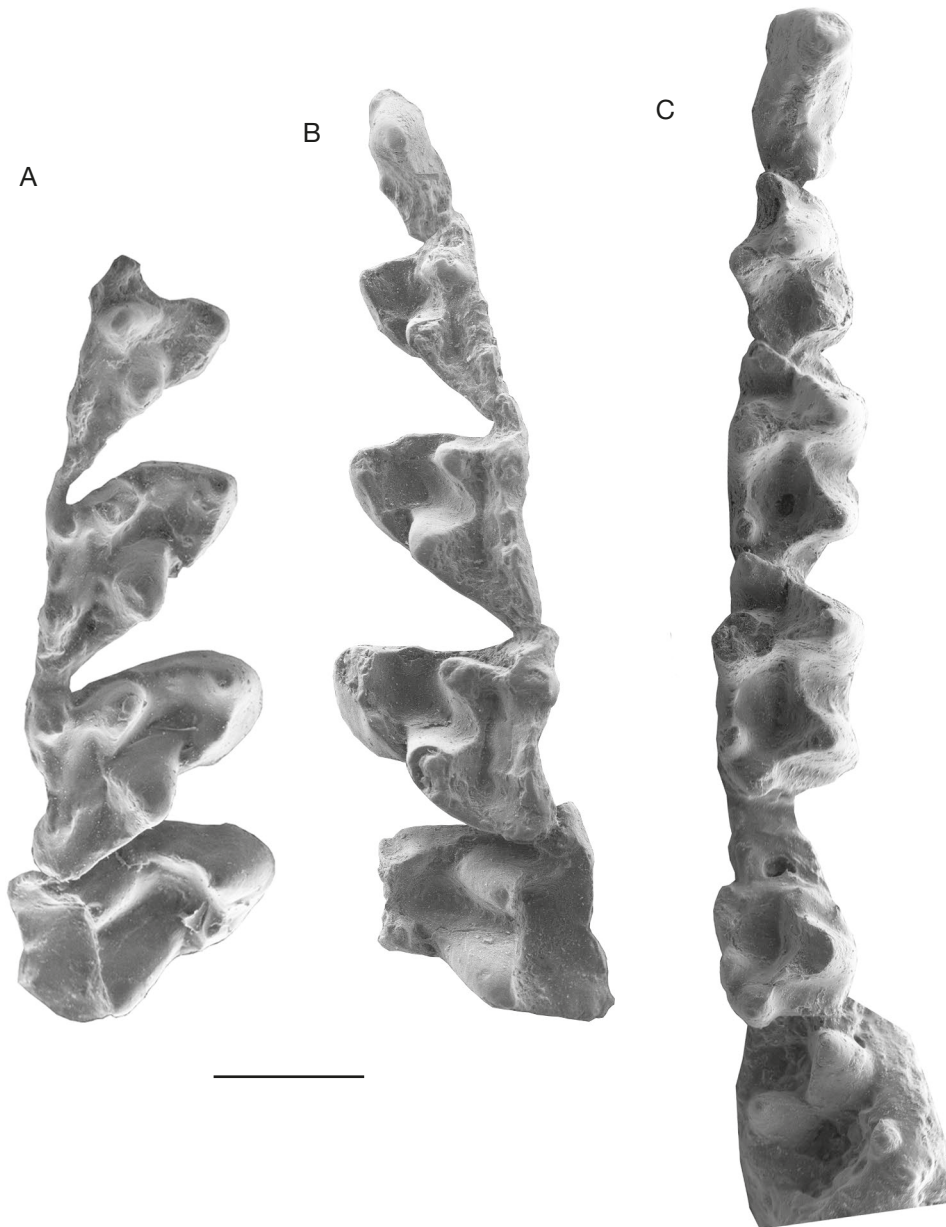


FIG. 2. — *Incadelphys antiquus*, holotype, YPFB Pal 6251 (SEM photo of cast): **A**, left maxillary with P1-P2, dP3, M1-M2; M3, missing the protocone, erupting; **B**, right maxillary with dP3, M1-M2, M3 erupting; **C**, right dentary with p3, dp3, m1-m2, m3 missing the trigonid, m4 in crypt. Scale bar: 1 mm.

(in pucadelphyids it is generally as long as or shorter than talonid of m4); lower molars proportionally narrower; entoconid proportionally larger, slightly higher as compared to hypoconid (in pucadelphyids the entoconid is approximately as high as the hypoconid).

Incadelphys antiquus differs from *Aenigmadelphys archeri* in that the paracone is slightly smaller in height and volume than the metacone (reversed in *A. archeri*); paraconule subequal to metaconule (in *A. archeri* paraconule is larger than metaconule); ectoflexus absent on M1 (present and shallow in *A. archeri*); anterior styler shelf narrower than posterior (in *A. archeri* the anterior styler shelf is wider than the posterior on the holotype only [an M3], but it is narrower on OMNH 23460, [an M3 lacking the protocone], OMNH 20120 [an M2], and OMNH 22898 [an M1]); styler cusp B and D subequal in size (in *A. archeri* styler cusp B is consistently larger than D); styler cusp C absent on M3 (in *A. archeri* it is small but distinct); trigonid lower as compared to talonid; paraconid distinctly smaller than metaconid (in *A. archeri* paraconid is subequal in size to metaconid or slightly smaller).

HYPODIGM. — The holotype; MHNC 13906, anterior half of a skull including both premaxillae, maxillae, nasals, lacrimals, anterior part of the frontals, anterior part of the jugals, right I3-M4, left I1-M4 (crown of I1-2 broken at base; labial edge of styler shelf of M3-4 missing); left dentary (missing coronoid process) with i1-m4; right dentary with i2-m4 (labial edge of protoconid of m1-m3 abraded, associated to the skull, the specimen also includes seven caudal vertebrae, three metacarpals and three metatarsals; MHNC 13947, a partial maxilla with M1-M3; MHNC 8270, a left mandible, with c-m3 and alveoli of m4 (on molars lingual edge of para- and metaconid is scratched), MHNC 13933, a left M2, MHNC 13935, a left M2.

GEOLOGICAL SETTING AND AGE. — All the specimens of *Incadelphys antiquus* are from beds of the Santa Lucía Formation at Tiupampa and have been discovered in the locality called “the Quarry” by Gayet *et al.* (1992) and Marshall & Muizon (1995). As discussed by



FIG. 3. — *Incadelphys antiquus*, MHNC 13906, partial skull with dentaries: **A**, ventral view; **B**, dorsal view; **C**, left lateral view; **D**, right lateral view; **E**, right dentary in lateral view; **F**, left dentary in lateral view. Scale bar: 5 mm.

Gelfo *et al.* (2009), Muizon *et al.* (2015, 2018), Muizon & Ladevèze (2020), the age of the Tiupampa beds is regarded as early Danian in age (*c.* 65 Ma) *contra* Zimicz *et al.* (2020).

COMPARATIVE DESCRIPTION

The new specimen of *Incadelphys antiquus* described here is an anterior part of a skull including the upper tooth rows and the palate, and both dentaries (Fig. 3). The specimen has suffered some distortion and the left maxilla has been displaced dorsally. In spite of this distortion, it seems that the width of the rostrum has not been strongly affected. The specimen includes the premaxillae, the maxillae, the lacrimals, the nasals, the anterior part of the frontals and jugals. The dentaries

are almost complete with all their teeth. However, during collection of the specimen, the lateral side of the left tooth rows have been damaged; on upper teeth, the posterolabial angle of M3 and the labial edge of the styler shelf of M4 have been destroyed. On the lower teeth, the labial edge of the protoconid and hypoconid of m1–m3 have been scratched during the collection of the specimen.

Dentition

The dental formula is the plesiomorphic pattern for metatherians: I5/i4, C/c, P3/p3, M4/m4 (Kielan-Jaworowska *et al.* 2004). The upper dentition will be described first, followed by the lower dentition.

TABLE 1. — Measurements of the teeth of *Incadelphys antiquus*. Abbreviations: **H**, height of the tooth; **Htl**, height of the talonid; **Htr**, height of the trigonid; **L** (for canines and premolars), maximum length of the tooth; **L** (for molars), maximum length of the tooth measured parallel to the paracone-metacone axis; **Lab**, length of the tooth along the labial alveolar border; **Lde**, length of the tooth along distal edge; **Lme**, length of the tooth along mesial edge; **Ltl**, length of the talonid; **Ltr**, length of the trigonid; **W** (for molars), maximum width of the tooth perpendicular to length; **W** (for canines and premolars), maximum width of the tooth; **Wtl**, maximum width of the talonid; **Wtr**, maximum width of the trigonid. Measurements are in mm.

Specimen	MHNC 13906		MHNC 13931		YPFB Pal 6251		Specimen	MHNC 13906		MHNC 13931		YPFB Pal 6251	
	Left	Right	Left	Right	Left	Right		Left	Right	Left	Right	Left	Right
L C	1.49	1.35	–	–	–	–	L p3	1.25	1.23	–	–	–	–
W C	0.65	0.65	–	–	–	–	W p1	0.33	0.34	–	–	–	–
H C	3.26	–	–	–	–	–	W p2	0.46	0.51	–	–	–	–
L P1	1.05	0.93	–	0.81	–	–	W p3	0.6	0.66	–	–	–	–
L P2	1.27	1.34	–	1.16	–	–	H p1	0.56	0.47	–	–	–	–
L P3	1.3	1.56	–	–	–	–	H p2	–	–	–	–	–	–
W P1	0.27	0.3	–	0.26	–	–	H p3	–	1.25	–	–	–	–
W P2	0.40	0.40	–	0.38	–	–	L d3	–	–	–	–	–	1.23
W P3	0.63	0.58	–	–	–	–	Ltr d3	–	–	–	–	–	0.64
H P1	0.81	0.84	–	0.68	–	–	Ltl d3	–	–	–	–	–	0.61
H P2	–	1.1	–	1.04	–	–	Wtr d3	–	–	–	–	–	0.68
H P3	1.3	–	–	–	–	–	Wtl d3	–	–	–	–	–	0.69
L D3	–	–	–	1.34	1.2	–	Htr d3	–	–	–	–	–	0.86
Lab D3	–	–	–	1.41	1.48	–	Htl d3	–	–	–	–	–	0.48
Lme D3	–	–	–	0.9	0.95	–	L m1	1.61	1.61	–	–	1.56	1.45
Lde D3	–	–	–	1.3	1.46	–	L m2	–	1.63	–	–	1.67	1.58
W D3	–	–	–	1.1	1.4	–	L m3	1.72	1.66	–	–	1.67	–
L M1	1.66	1.55	1.62	1.53	1.44	–	L m4	1.68	1.64	–	–	–	–
L M2	1.6	1.58	–	1.4	1.32	–	Ltr m1	0.94	0.97	–	–	0.85	0.92
L M3	1.58	1.56	–	–	1.39	–	Ltrm2	–	0.95	–	–	0.93	0.88
L M4	–	1.35	–	–	–	–	Ltr m3	0.97	0.93	–	–	0.83	–
Lab M1	1.72	1.65	–	1.6	1.51	–	Ltr m4	0.84	0.81	–	–	–	–
Lab M2	1.61	1.57	1.57	1.42	1.36	–	Ltl m1	0.53	0.67	–	–	0.68	0.7
Lab M3	–	1.58	–	1.49	–	–	Ltl m2	–	0.72	–	–	0.82	0.7
Lab M4	–	1.41	–	–	–	–	Ltl m3	0.66	0.71	–	–	0.8	0.89
Lme M1	1.24	1.34	–	1.29	1.39	–	Ltl m4	0.79	0.7	–	–	–	–
Lme M2	1.67	1.67	–	1.55	1.68	–	Wtr m1	0.7	–	–	–	0.85	0.86
Lme M3	1.62	1.87	1.33	–	2.02	–	Wtr m2	–	–	–	–	0.9	0.96
Lme M4	–	1.96	–	–	–	–	Wtr m3	0.96	–	–	–	1.03	–
Lde M1	1.68	1.84	1.78	1.66	1.93	–	Wtr m4	0.84	0.91	–	–	–	–
Lde M2	1.67	1.93	–	1.85	2	–	Wtl m1	0.7	–	–	–	0.85	0.82
Lde M3	–	2.06	–	–	2.08	–	Wtl m2	–	–	–	–	0.85	0.89
Lde M4	–	1.3	–	–	–	–	Wtl m3	0.83	–	–	–	1.02	0.88
W M1	1.41	1.60	1.52	1.51	1.7	–	Wtl m4	0.69	0.78	–	–	–	–
W M2	1.58	1.69	–	1.78	1.91	–	Htr m1	0.85	–	–	–	0.96	0.81
W M3	–	1.91	–	–	2	–	Htr m2	–	1.12	–	–	1.1	1.01
W M4	–	1.78	–	–	–	–	Htr m3	1.29	1.32	–	–	1	–
L c	1.2	1.1	–	–	–	–	Htr m4	1.25	–	–	–	–	–
W c	0.58	0.65	–	–	–	–	Htl m1	0.45	0.46	–	–	0.4	0.44
H c	1.7	1.9	–	–	–	–	Htl m2	0.55	0.54	–	–	0.55	0.53
L p1	0.89	0.97	–	–	–	–	Htl m3	0.6	0.86	–	–	–	0.67
L p2	1.25	1.36	–	–	–	–	Htl m4	0.52	–	–	–	–	–

Upper dentition

Upper incisors (Figs 4; 5). the crowns of I1 and I2 are missing and the roots of these teeth are preserved only on the left premaxilla. I1 has a slightly smaller diameter than I2. This condition contrasts with that of extant didelphids and *Andinodelphys*, in which I1 is distinctly larger than I2. In contrast, it resembles the condition observed in the only *Pucadelphys* specimens that preserve the I1s (YPFB Pal 6105, the holotype, and MHNC 8378, referred to females by Ladevèze *et al.* 2011). A small diastema is present between I1 and I2. The diastema is approximately as long as the diameter of I1. A similar condition is present in some specimens of *Pucadelphys* (MHNC 8378) and in didelphids but is absent in *Andinodelphys*. The crowns of the other incisors are preserved. They are subequal in size to I2, with I5 being slightly smaller. Their

crown is peg-like. It is slightly compressed labiolingually on I3 and I4 and roughly conical on I5.

Upper Canine (Figs 4; 5). The upper canine is large and sharp and is approximately three times as high as the P3. It is larger than in *Marmosa*, in which it is twice as high as P3, and *Thylamys*, in which it is less than twice the high of P3. It is similar in height to the canines of *Didelphis* and *Caluromys*, in which they are approximately three times (or more) as high as the P3. Among the Tiupampa metatherians, the canine of *Incadelphys* is similar in relative height to those of *Andinodelphys* and specimens interpreted by Ladevèze *et al.* (2011) as males of *Pucadelphys* (e.g., MHNC 8266, 8377, 8382). In contrast, it is clearly higher than the canines of the specimens referred to females of *Pucadelphys* by these authors (e.g., MHNC 8376, 8378), in

which the canine height is less than twice that of P3. As in all didelphids and pucadelphyids, the upper canines of *Incadelphys* are transversely compressed being approximately twice as long as wide. As in didelphids and pucadelphyids, they are strongly curved posteriorly. The upper canine of *Incadelphys* is slightly procumbent as indicated by the position of the apex of the tooth, which is ventral to the anterior edge of the crown base.

Upper premolars (Figs 4; 5). The three premolars are double-rooted and distinctly increase in size from P1 to P3. As observed on the right side of the skull, the increase in size is progressive. In other words, the increase in size between P1 and P2 is similar to that between P2 and P3. This condition differs from that observed in *Andinodelphys*, in which a great increase in size is observed between P1 and P2 and a smaller increase exists between P2 and P3. A small diastema is present between P1 and P2, and a smaller one between P2 and P3. P1 and P2 are extremely narrow transversely and blade-like, whereas P3 is slightly wider (Table 1). The blade-like morphology of the P1-P2 is not observed in any of the other Tiupampa metatherians. As shown on Table 2 the ratio W/L for the P2 of *Incadelphys* is 0.31 (three measurements), 0.45 for *Andinodelphys* (seven measurements), and for *Pucadelphys* 0.56 (ten measurements). Therefore, the relative width (as compared to length) of the P2 of *Incadelphys* is 31% smaller than in *Andinodelphys* and 45% smaller than in *Pucadelphys*. Given these results, the blade-like morphology of the anterior upper premolars of *Incadelphys* is regarded as a significant characteristic of the genus. P1 is triangular in lateral view. It is slightly asymmetrical, with its apex located below the anterior root. It is less asymmetrical than in *Andinodelphys*, in which the apex of P1 is ventral to the posterior edge of the posterior root. The P1 of *Incadelphys* has no posterior accessory cusp, nor cingulum. Its anterior root contacts the posterior edge of the canine, but it is not closely appressed against it, thus differing from the condition of *Andinodelphys*. P2 is less asymmetrical than P1 and its apex is ventral to the inter-alveolar septum. Similarly to P1, it is as long as high. Its anterior and posterior edges are straight. The tooth bears a small cingulum at the anterior edge of the crown, which forms a hint of an anterior basal cuspule. The cingulum extends on the lingual aspect of the crown, below the anterior root. Posteriorly a conspicuous basal cusp is present. P3 is more robust and more inflated than P2. Its anterior edge is slightly convex and its posterior edge slightly concave. The apex of the crown is located below the anterior edge of the posterior root. The anterior border of the crown is rounded, whereas the posterior edge becomes thinner, sharp, and crest-like. The lateral edges of the crown, in this region, are distinctly concave. The anterior cingulum is strong (as compared to that of P2). It extends on the mesiolabial and mesiolingual angles of the crown but remains at the level of the anterior root. Posteriorly, the basal accessory cusp is well developed. It imbricates in the mesiolingual angle of M1 with the stylar cusp A. Labial and lingual to the basal cusp are small cingular shelves.

Upper molars (Figs 4; 5). The description of the upper molars will consider the five available specimens: the holotype YPFB

TABLE 2. — Proportions of P2 in some Tiupampa metatherians.

Specimen	Length of P2	Width of P2	Width/Length
<i>Incadelphys</i>			
YPFB Pal 6251	1.19	0.38	—
MHNC 13906 Right	1.34	0.4	—
MHNC 13906 Left	1.27	0.4	—
Mean	1.26	0.39	0.31
<i>Andinodelphys</i> (mean of seven measurements; see Muizon & Ladevèze 2020: Table 2)			
	2.21	0.99	0.45
<i>Pucadelphys</i>			
YPFB Pal 6105	1.4	0.9	—
YPFB Pal 6109	1.5	0.9	—
MHNC 8266	1.51	0.72	—
MHNC 8376	1.26	0.69	—
MHNC 8377	1.38	0.78	—
MHNC 8378	1.43	0.72	—
MHNC 8379	1.48	0.79	—
MHNC 8380	1.53	0.88	—
MHNC 8381	1.51	0.91	—
MHNC 8382	1.42	0.78	—
Mean	14.4	0.8	0.56

Pal 6251, which includes both maxillae and mandibles of a subadult individual (i.e. upper M4 are missing and m4 are unerupted); MHNC 13906 (which preserves complete maxillae and mandibles and 13931 a partial maxilla with M1-3). M1 is relatively different from the other molars and will be treated first. M2-M3, which have a more typical morphology as compared to most of the other Tiupampian metatherians will be described jointly. M4, which strongly differs from the preceding molar, as in most metatherians, will be studied next.

M1 is a distinctive tooth of *Incadelphys* in the distolabial extension of its metastylar angle. As a consequence, the labial edge of M1 is much longer than on the other molars (Table 1). The anterior edge is shorter than on the posterior molars, and the tooth is longer than wide (1.56 mm vs 1.54mm; mean of five measurements, see Table 1), a condition that contrasts with that of *Andinodelphys*, *Pucadelphys*, and *Mizquedelphys*. A condition of the M1 similar to that of *Incadelphys* is observed in the Campanian genus *Aenigmadelphys* of Utah. Table 3 compares the angle between the line joining stylar cusps D and E and the postmetacrista. Because the postmetacrista is often curved, and because the posterolabial part of the crista is relatively straight, the latter has been used for the measurement. As observed in Table 2, the mean of the angle obtained for pucadelphyids (53.2°) is approximately 48% and 32% greater than the angle of *Incadelphys* and *Aenigmadelphys* respectively. Because of this difficulty of measurement, the value of the angle obtained is certainly somewhat imprecise. However, because of the great difference observed, this result is probably significant. As a consequence of the posterolabial extension of the M1, its mesial edge is distinctly shorter than its labial edge. A similar condition is also observed in *Aenigmadelphys*. *Marmosopsis* from the early Eocene of Itaboraí, clearly ranges close to *Incadelphys*, whereas *Monodelphis* and *Thylamys* are closer to pucadelphyids than to *Incadelphys* and *Aenigmadelphys*.



FIG. 4. — *Incadelphys antiquus*, MHNC 13906: A, stereopair of the right maxilla and upper tooth row in occlusal view. Scale bar: 5 mm.

The protocone of M1 is relatively massive, being mesiodistally longer than wide on the three specimens. It is roughly symmetrical mesiodistally and does not present the distolingual inflation observed in didelphids and pucadelphyids. The mesial and distal bases of the protocone are smooth and bear no cingulum. Para- and metaconules are well-developed

(almost as large as styler cusps B and D). From the paraconule, a conspicuous paracingulum (i.e. labial extension of the preparaconular crista) extends up to styler cusp A. Distally, the metaconule abuts the distal base of metacone but no metacingulum (i.e. labial extension of the postmetaconular crista) is present. The paracone is slightly smaller



FIG. 4. — *Incadelphys antiquus*, MHNC 13906: **B**, stereopair of the left maxilla and upper tooth row in occlusal view. Scale bar: 5 mm.



FIG. 5. — *Incadelphys antiquus*, MHNC 13906: **A**, lateral view of the right upper tooth row; **B**, lateral view of the left upper tooth row. Scale bar: 5 mm.

in height and volume than the metacone. Both cusps are widely separated at base, as in didelphids and pucadelphyids. A deep trigon basin is bordered by the distolingual aspect of the paracone, the mesiolingual aspect of the metacone and the labial aspect of the protocone. The lingual aspect of the para- and metacone is strongly convex, whereas their labial aspect is flat to slightly concave. As a consequence, the cusps are triangular in section and the pre- and post- paracristae and pre- and post-metacristae are shifted labially, forming the lingual wall of the stylar shelf. The junction of the postparacrista and premetacrista (i.e. the median point of the centrocrista) is displaced labially, and the centrocrista is slightly V-shaped in occlusal view. This condition, which is present in *Aenigmadelphys*, didelphids, and pucadelphyids, differs from that observed, for instance, in *Kokopellia*, alphadontids, peradectids, and sparassodonts, in which the labial and lingual aspects of the para- and metacone are markedly convex (generally slightly less convex labially than lingually), the pre- and post- paracristae and pre- and post-metacristae are in a median position relative to the para- and metacone and therefore the centrocrista is straight. The stylar shelf of *Incadelphys* is narrow, being almost absent anteriorly since the stylar cusp B is almost connate to the paracone to which it is connected by a very short preparacrista. The stylar cusp A is smaller than B but conspicuous. It surrounds posterolabially and imbricates with the posterobasal cusp of P3. Stylar cusp B and D are large and subequal in size, but variation exists. In MHNC 13906, StB is slightly smaller than StD, whereas in MHNC 13931 StB is slightly larger than StD; these cusps

are subequal in the holotype. Stylar cusp B is conical, whereas stylar cusp D is transversely compressed. Between StB and StD, a small stylar cusp C is present in the holotype and MHNC 13906. Stylar cusp C is lacking in MHNC 13931. Stylar cusp E is indistinguishable. The labial edge of M1 is straight and features no ectoflexus.

M2 and M3 are conspicuously wider than long. They differ from M1 in the protocone, which is approximately as long as wide on M2 and clearly wider than long on M3. The stylar shelf is wider than on M1, especially its anterior part. As a consequence, the stylar cusp B is well separated from the paracone, and the preparacrista is as long as the postparacrista on M2 and slightly longer on M3. The preparacrista contacts stylar cusp B on its anterior edge, almost between cusp B and A on MHNC 13906. Stylar cusp C is small to absent and stylar cusp D is well developed but smaller than B. On the labial edge of M2 is a small ectoflexus (rather a notch) between stylar cusps B and C. On M3, the ectoflexus is deeper and located between stylar cusps C and D. From M1 to M3, at the distolabial corner of the tooth, the angle between the labial edge and the postmetacrista increases and, as a consequence, the postmetacrista is more transverse posteriorly. M2-M3 of *Incadelphys* strongly resemble those of *Aenigmadelphys*, from which they differ however in the latter being transversely wider and mesiodistally shorter (see comparison below p. 000). Furthermore, the M2-M3 of *Aenigmadelphys* have a slightly wider stylar shelf.

On M4, the protocone is shorter mesiodistally than on the anterior molars and the metacone is greatly reduced compared

TABLE 3. — Comparison of the distolabial angle of M1 in *Incadelphys*, *Aenigmadelphys*, pucadelphyids, *Szalinia*, *Marmosopsis*, *Derorhynchus* and two extant didelphids. The angle is measured between the distolabial edge of the tooth (roughly, the line joining the styler cusp E or styler cusp E position and styler cusp D) and the postmetacrista. Because the postmetacrista is generally curved (being concave mesiolabially), the posterior half of the crista (which is straighter) has been considered, rather than the full crista. Because of this bias, the angles measured are approximate. Nevertheless, the great difference observed between *Incadelphys*, *Aenigmadelphys*, and *Marmosopsis* on the one hand and pucadelphyids on the other is regarded here as significant. When two values are provided for a given specimen they refer to the right and left M1.

<i>Incadelphys antiquus</i>	YPFB Pal	MHNC	MHNC							Mean
specimens	6251	13906	13931							
angle	36°	37°, 36°	35°							36°
<i>Aenigmadelphys archeri</i>	OMNH									
specimens	22898									
angle	39°									39°
<i>Pucadelphys andinus</i>	YPFB Pal	MHNC	MHNC	MHNC	MHNC	MHNC	MHNC	MHNC	MHNC	
specimens	6105	8266	8376	8377	8378	8379	8380	8381	8382	
angle	50°, 53°	50°, 58°	49°, 52°	58°	62°	51°	54°	60°	51°	51.4°
<i>Andinodelphys cochabambensis</i>	MHNC	MHNC	MHNC							
specimens	13847	8264	8370							
angle	59°	58°	58°							58.3°
<i>Mizquedelphys plipinensis</i>	YPFB Pal	MHNC								
specimens	6196	13917								
angle	49°	51°								50°
Mean for pucadelphyids										53.2°
<i>Szalinia gracilis</i>	MHNC									
specimen	8350									
angle	59°									59°
<i>Marmosopsis juradoi</i>	MNRJ	MNRJ	MNRJ	MNHN.F.						
specimens	2478-V	2481-V	2482-V	ITB 83						
angle	41°	37°	41°	36°						39°
<i>Derorhynchus singularis</i>	DGM									
specimen	803-M									
angle	49°									49°
<i>Monodelphis</i> spp.	2003-762		2004-317		1967-330					
specimens	<i>M. brevicaudata</i>		<i>M. brevicaudata</i>		<i>M. domestica</i>					
angle	49°		46°		53°					49.3°
<i>Thylamys</i> sp.	CM pers									
specimen	coll									
angle	47°									47°

to that of the anterior molars, being significantly smaller than the paracone. The anterior styler shelf is wider and the preparacrista is longer than on M2-M3. The posterior styler shelf is very narrow but still present labial to the metacone. The M4 of *Incadelphys* differs from that of *Aenigmadelphys* in the latter being mesiodistally shorter, transversely wider with a longer preparacrista, and in the posterior styler shelf being virtually absent.

Lower dentition

Lower incisors (Figs 6; 7). The four incisors are preserved on the left dentary, but i1 is missing part of its crown. In the description below, we follow the interpretation of Hershkovitz (1982, 1995), that the four lower incisors of metatherians are serially homologous to i2-i5. On the right dentary i2-i4 are preserved but i5 is missing its crown. In size, the crown of i2 is smaller than that of i3 but larger than i4; i5 is the smallest of the four incisors. The crowns are peg-like but slightly spatulate, being wider than high. The apex of the crown of i2 is roughly semicircular in labial or lingual view; that of i3 is lanceolate with a carina on its lingual aspect; that of i4

is similar to i1 but smaller and that of i5 is also somewhat lanceolate. The i3 is distinctly staggered as indicated by the buttress visible on the anterolabial edge of the dentary just ventral to the labial aspect of the tooth and by the posterior shift of its root observable lingually on MHNC 13906.

Lower canine (Figs 6; 7). The lower canine is a large tooth, although consistently smaller than the upper canine. It is pointed at its apex and curved (from the alveolar border) dorsally but not posteriorly. In other words, the apex of the tooth does not overhang the distal edge of the crown, which is procumbent (Fig. 7). The canine is slightly recurved lingually, this feature being more pronounced on the right dentary. Its anterior edge is closely appressed against the posterior edge of i5.

Lower premolars (Figs 6; 7). The lower premolars are well preserved on MHNC 13906. From p1 to p3 the lower premolars of *Incadelphys* conspicuously shift from a mesially tilted to an upright position. The p1 is very small and procumbent, being strongly asymmetrical in lateral view. Its apex is strongly shifted mesially and overhangs the anterior



FIG. 6. — *Incadelphys antiquus*, MHNC 13906: **A**, stereopair of the left lower tooth row in occlusal view; **B**, stereopair of the right lower tooth row in occlusal view. Scale bar: 5 mm.

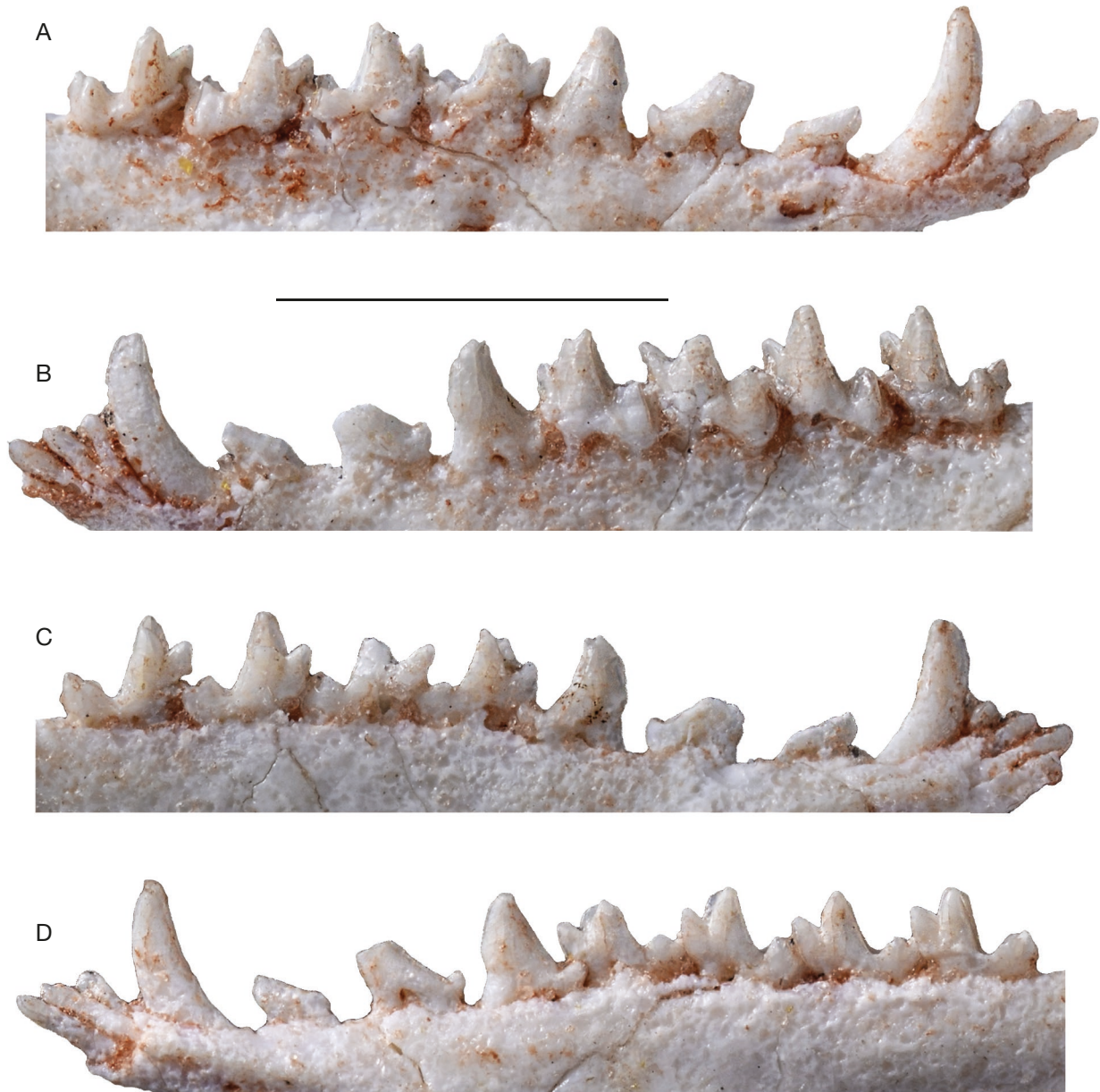


FIG. 7. — *Incadelphys antiquus*, MHNC 13906: **A**, lateral view of the right lower tooth row; **B**, medial view of the right lower tooth row; **C**, lateral view of the left lower tooth row; **D**, medial view of the left lower tooth row. Scale bar: 5 mm.

edge of the anterior root of the tooth. As a consequence, the posterior edge of the tooth is very long and strongly oblique. It is straight and bears no cuspule at its distoventral end. The anterior edge of the crown is markedly convex and extends mesially over the posterior edge of the canine. This highly asymmetrical morphology of the p1 of *Incadelphys* resembles that observed in *Szalinia*, in *Andinodelphys*, in most specimens of *Pucadelphys*, and in *Marmosopsis*. It is also present in *Monodelphis* and *Marmosa*. A small (approximately half the length of p1) diastema separates p1 and p2; a diastema half as long separates p2 from p3. The p2 is larger than p1 being intermediate in size between the latter and p3. It is also strongly shifted anteriorly but less procumbent than p1. Because its apex is missing on both sides, its position relative to the root

cannot be evaluated precisely. It is clear, however, that it was overhanging the anterior root of the tooth. The anterior edge is strongly convex and projects anterior to the anterior edge of the anterior root. The posterior edge is straight and bears a sharp and pointed accessory cusp at its distoventral end. The p3 is robust and roughly as high as long. It is subvertical, not procumbent, and its apex overhangs the middle region of the anterior root. The anterior edge of the tooth is subvertical but still convex anteriorly and projects above the anterior edge of the anterior root. The posterior edge of p3 is longer than the anterior but relatively less, as compared to anterior premolars. It is slightly concave dorsally and bears a large accessory cusp at its base. None of the premolars bears any kind of cingulum.

Lower molars (Figs 6; 7). The lower molars slightly increase in length distally from m1 to m3. The m4 is slightly shorter than the preceding tooth. The length of the trigonid decreases posteriorly from m1 to m4. On the four molars, the trigonid is more than two times as high as the talonid. The trigonid of m1 is relatively long with a paraconid set mesiolabially (as compared to the other molars) so that the angle between the paracristid and protocristid is more open lingually. As a consequence, the trigonid of m1 is distinctly longer than wide, while it is approximately as wide as long on m3-4 (measure not available on m2). The protoconid is the largest cusp of the trigonid; it is triangular in section, while the metaconid is roughly ovoid and less voluminous. In lingual view, the metaconid is subvertical and slightly decreases in length distally; its posterior edge is sloping on m1 and becomes subvertical on m4. The paraconid is the smallest cusp of the trigonid. In lingual view, it is consistently tilted mesially, a condition that reduces on posterior molars.

Paraconid and metaconid are connate at base, and the valloid between them is higher than half of the metaconid height (measured from the lingual alveolar border). Because of this condition, the trigonid basin is elevated, well-excavated, and well-circumscribed lingually at least on m2-4. On these molars, the deepest point of the basin is at the level of, or lower than, the uppermost point of the paraconid-metaconid vallid. This condition is similar to that observed in *Pucadelphys* but differs distinctly from that observed in the Tiupampa sparassodonts, *Mayulestes* and *Allqokirus*. In these taxa, the paraconid and metaconid are broadly separated and the valloid between them is wider and extends almost as far as the base of the crown lingually. As a consequence, the trigonid basin of these sparassodonts is broadly open lingually and is more a slope on the lingual side of the protoconid than a true depression. The paraconid of *Incadelphys* is triangular in section and its mesiolingual angle bear a moderately salient paraconid ridge. Labial to this ridge is a shallow hypoconulid notch. The paracristid and protocristid are sharp but bear no carnassial notch. The median point of the cristids (the point of contact of the cusps) is slightly lower on the paracristid than on the protocristid, this condition being more marked on the anterior molars. The paracristid is strongly oblique relative to the axis of the tooth row, whereas the protocristid is slightly oblique on m1-m2 and distinctly transverse on m3-m4. The angle of the paracristid with the axis of the tooth row increases from m1 to m4.

The talonid is distinctly basined. On m1-3, the hypoconid is the largest cusp in height and volume; the entoconid and the hypoconulid are subequal in height and volume. On m4, the hypoconulid is the highest cusp of the talonid and is almost as voluminous as the hypoconid. It is consistently larger than the entoconid. The hypoconid is large and occupies approximately half of the talonid volume. It is conspicuously larger than the other cusps of the talonid. In occusal view, it is triangular to V-shaped in appearance. At the mesial edge of the hypoconid, the cristid obliqua is well-developed and sharp. It extends mesiolingually and connects to the trigonid at the distolingual edge of the protoconid (i.e. slightly

labial to the protocristid notch). On the distolingual edge of the hypoconid, a strong posthypocristid connects to the hypoconulid. It is distolabially concave and deeply notched between the two cusps. The posthypocristid notch is located approximately at midline of the talonid. At the distolingual angle of the talonid, the hypoconulid and entoconid are distinctly connate. The hypoconulid is lingual to the midline of the talonid. The entoconid is larger than the hypoconulid on m1-m2, subequal to hypoconulid on m3, and smaller on m4. On its mesial edge, it bears, a marked entocristid, which connects the distal base of the metaconid. Therefore, the talonid is relatively well enclosed lingually. On m4, the hypoconulid is enlarged and elevated above the other talonid cusps. The entoconid is reduced and partially fused at the base of the hypoconulid. A well-developed precingulid is present at the mesial base of the protoconid and extends on the mesiolabial base of the paraconid. A thick postcingulid is present on distal edge of m1-3 as a shelf extending ventrolabially from the apex of the hypoconulid to the distal edge of the hypoconid as far as its labial side. A postcingulid is absent on m4.

Bony skull

General features. Because the skull of *Incadelphys antiquus* described here is incomplete, little can be described of its general features. However, the presence of diastemata between the upper and lower premolars is an indication of a relatively elongated rostrum, as observed in the male specimens of *Pucadelphys* (Ladevèze *et al.* 2011); the rostrum of *I. antiquus* was probably also approaching the condition observed in the extant species of *Thylamys*, but it was not as long, relatively, as that of *Andinodelphys*. Furthermore, in spite of the rostrum distortion and displacement of the maxillae and premaxillae, it is possible to observe that the apex of the snout was slender and narrow, as in *Pucadelphys* and *Thylamys*.

Premaxilla (Figs 8; 9). In lateral view the premaxilla presents a long and narrow posterodorsal process (the facial process), which is wedged between the nasal and the maxilla. The apex of the process extends posteriorly as far as the posterior third of the parallel-sided anterior portion of the nasal. On the lateral aspect of the rostrum, the premaxilla-maxilla suture is roughly straight. Anteroventrally the suture reaches the alveolar border between I4 and I5. In other words, a small anterolateral process of the maxilla covers the premaxilla in the area of the lateral alveolar border of I5 (see below). The dorsal edge of the premaxilla forms a right angle at the junction of the part that articulates with the nasal and the lateral border of the narial opening. In lateral view, the premaxillae are consistently bent ventrally, to a greater extent than in any other extant didelphids and in pucadelphyids. This is especially clear on the right side of the specimen, which does not show cracks or distortion. On the left side a subvertical crack is observed anterior to the canine but apparently with no (or little) ventral displacement of the premaxilla. A similar condition is present in *Allqokirus* (Muizon *et al.* 2018), although the taxa do not appear to be closely related. In dorsal view, the anterior edge of the two premaxillae have a strongly convex

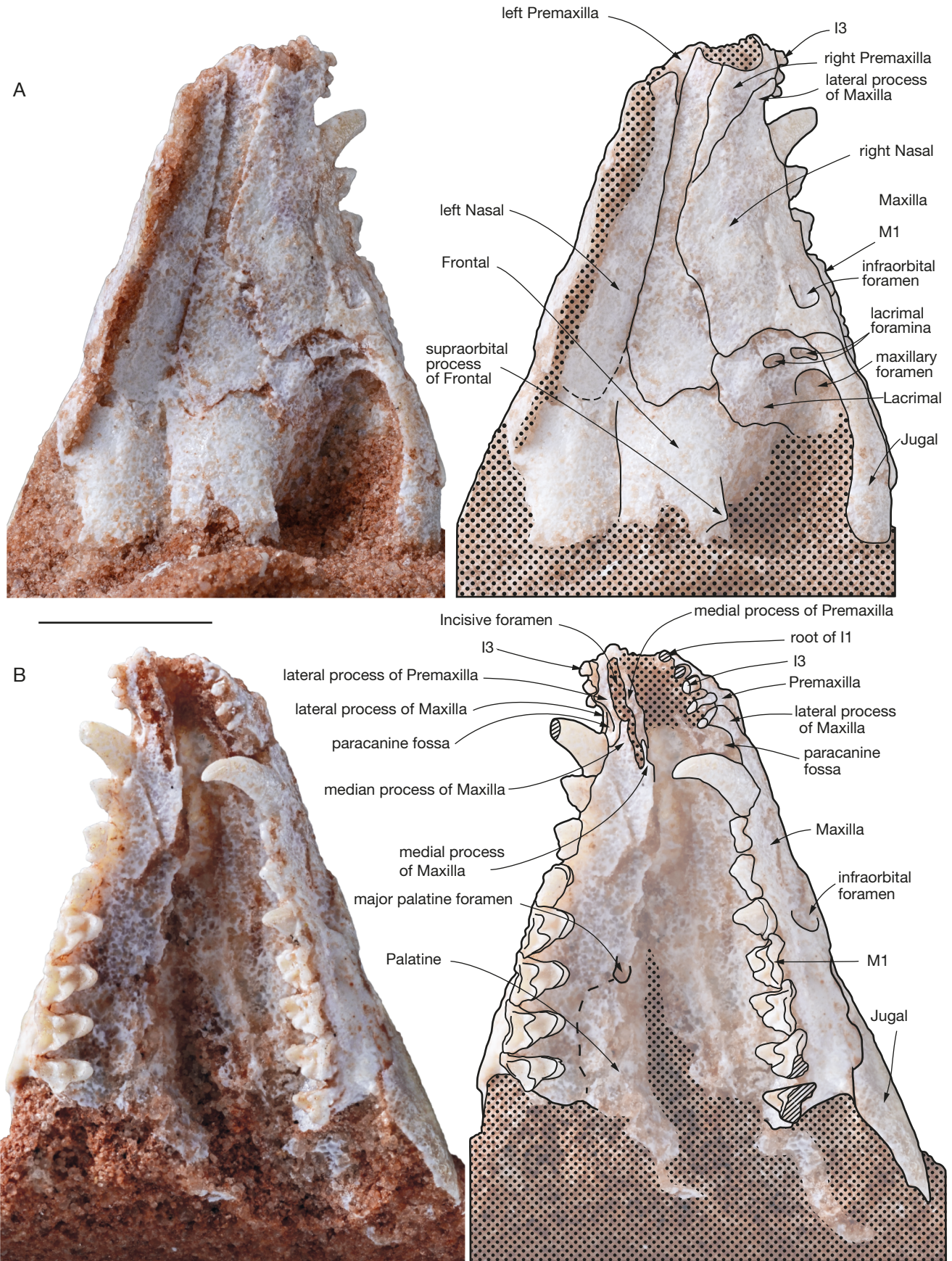


FIG. 8. — *Inca delphys antiquus*, MHNC 13906: **A**, dorsal view of the anterior skull; **B**, ventral view of the anterior skull. Scale bar: 5 mm.

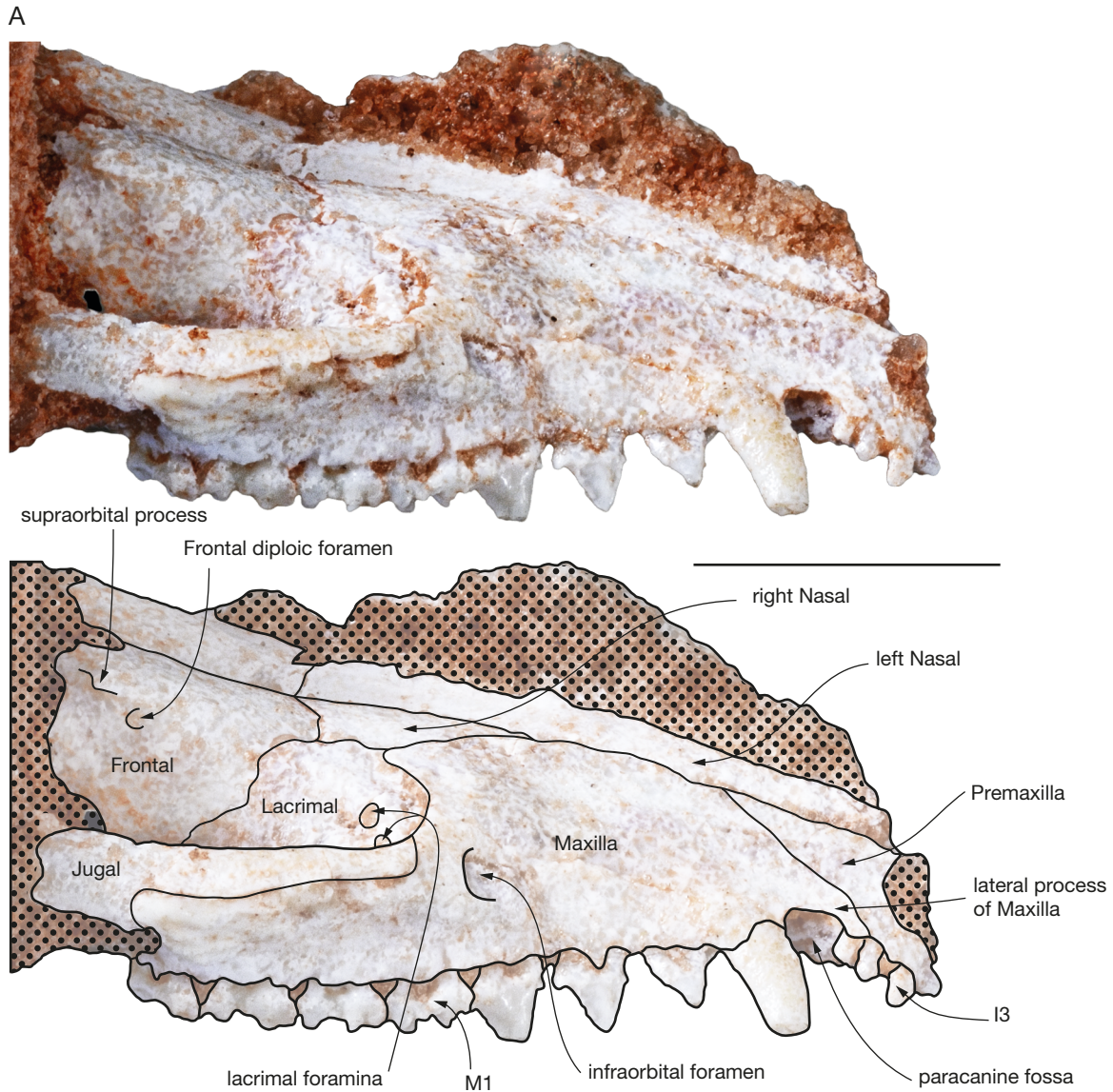


FIG. 9. — *Incadelphys antiquus*, MHNC 13906: A, left lateral view of the anterior skull. Scale bar: 5 mm.

shape (parabolic). The two premaxillae form approximately the portion of the palate anterior to the anterior alveolar border of the canines, with a small contribution of the anterolateral processes of the maxillae. On the palate, the premaxillae are pierced by the anterior half of the elongated incisive foramina (only observable on the right side). The ventral view of the premaxilla shows two posteriorly oriented branches, which form the lateral and medial edges of the incisive foramina. These branches articulate posteriorly with the maxilla on the palate. The lateral branch of the premaxilla, which borders the incisive foramen laterally, has approximately the same width from I1 to the canine. It is approximately as wide as the incisive foramen. Its posterior extremity is located between the anterolateral and the anteromedian processes of the maxilla (the latter being located between the anteromedial and anterolateral processes), (fig. 8B). The posterolateral branch of the premaxilla bears the medial two thirds of the para-

nine fossa for the lower canine, which is located just anterior to the upper canine. This branch is rounded posteriorly and contacts the anteromedial edge of the alveolus of the canine. In the anterior region of the paracanine fossa is the alveolus of the I5, while the fossa extends anteriorly as a narrow sulcus on the medial edge of the alveolar border of I5. In the posterior region of the paracanine fossa, the premaxilla-maxilla suture is V-shaped anteriorly. It enters the palate at the level of the posterolabial alveolar border of I5 (between the apex of the anterolateral process of the maxilla and the premaxilla), runs posteromedially from the lateral aspect of the rostrum, almost reaches the anteromedial edge of the canine alveolus, makes a V-turn, and extends further anteromedially as far as approximately the posterior half of the lateral edge of the incisive foramen. The medial branch of the premaxilla forms the medial edge of the incisive foramen for approximately 80% of its length anteriorly. This medial branch articulates

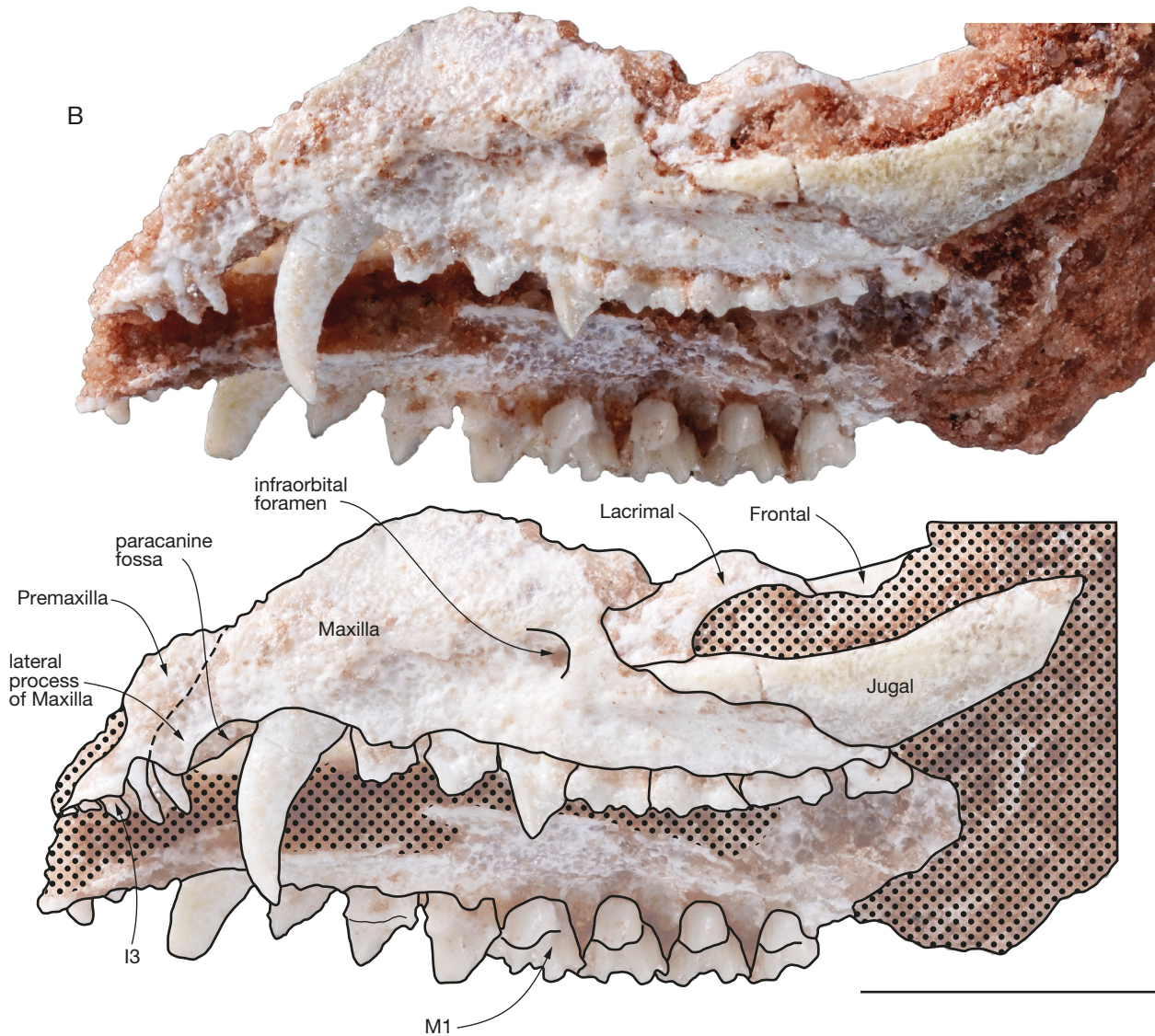


FIG. 9. — *Incadelphys antiquus*, MHNC 13906: B, right lateral view of the anterior skull. Scale bar: 5 mm.

posteriorly with a small anteromedial process of the maxilla and both structures slightly overlap anteroposteriorly. The medial branch is narrower than the lateral one.

The incisive foramen is anteroposteriorly elongated and narrow. It is approximately ten times narrower than long. It extends from a point medial to I3 anteriorly to a point medial to the posterior edge of the alveolus of the canine posteriorly.

Maxilla (Figs 8; 9). The maxilla forms the lateral wall of the rostrum between the posterodorsal process of the premaxilla and the lacrimal (which represents the facial process). Ventrally, it forms most of the palate between the premaxilla anteriorly and the palatine posteriorly (which represents the palatal process). Anteriorly, the maxilla presents an anterolateral process, which forms the lateral wall of the paracanine fossa between I5 and the canine. Its medial edge is excavated and forms the lateral third part of the fossa. The anterolat-

eral process of the maxilla overlaps the posterolateral edge of the premaxilla to a point labial to I5. Posterodorsally, the facial process of the maxilla forms a broad triangular process, which articulates dorsally with the nasal and ventrally with the lacrimal. It has no suture with the frontal and therefore a distinct lacrimal-nasal suture is present. From the apex of the posterior process, the maxilla-lacrimal suture runs in an anterior direction and turns anteroventrally along the anterior rim of the orbit to contact the jugal at the lower edge of the orbit, just anteroventral to the ventral lacrimal foramen. This triple point, which connects the maxilla, the lacrimal and the jugal, is dorsal to the posterior edge of M1. Posterior to this point, the maxilla has a long suture with the jugal, which extends posteriorly along the ventral edge of the jugal on the lateral face of the skull. At the level of the anterior end of the orbitotemporal fossa, the suture passes on the medial side of the zygomatic arch.

On the lateral aspect of the rostrum is a small anterior foramen of the infraorbital canal. It opens (dorsal to posterior edge of P3 and is at the level of the ventral lacrimal foramen dorsoventrally. Because of the distortion of the specimen it is not possible to evaluate the proportions of this foramen. The infraorbital canal transmits the infraorbital nerve (a branch of the V2) and the infraorbital artery, which innervate and supplies blood to the face respectively.

Anterodorsal to the alveolar border of the canine, the maxilla has a narrow anterior lateral process which forms the lateral edge of the paracanine fossa. The anterior end of the process contact the posterolabial angle of I4 (Fig. 9).

On the lateral aspect of the rostrum, ventral to the maxilla-jugal suture and dorsal to the alveolar border of M1-M3, is an elongated fossa which extends from a point dorsal to posterior edge of P3 to anterior edge of M3 (Fig. 9). A similar fossa has been observed in *Allqokirus australis* (Muizon *et al.* 2018) and *Andinodelphys cochabambensis* (Muizon & Ladevèze 2020) and has been interpreted as the origin of the *levator labii superioris* muscle. Such a fossa is also present in *Mayulestes* and *Pucadelphys*. In extant didelphids, the fossa for the *zygomaticus* and *levator labii superioris* is generally deep and well developed on the anterolateral region of the jugal but does not excavate the maxilla anterior to the jugal-maxilla suture, although the muscles also originate in part on the maxilla (Turnbull 1970). Because the origin of the *levator labii superioris* in *Didelphis* is ventral to that of the *zygomaticus*, it is likely that the fossa observed in *Incadelphys* and the other Tiupampa metatherians corresponds to the origin of the *levator labii superioris*, while the *zygomaticus* probably originated on the jugal as in *Didelphis*, although no fossa for this muscle is observed on the jugal of *Incadelphys*.

Ventrally, the maxilla forms most of the palate from the incisive foramen anteriorly to the maxilla-palatine suture posteriorly. Although in MHNC 13906 the palatal processes of the maxillae are badly crushed, some observations can be made. Anteriorly on the right maxilla the posterior end of the incisive foramen is preserved. In this region, the maxilla has a thin medial process which borders the incisive foramen posteromedially on its posterior fifth and joins the medial process of the premaxilla anteriorly. The posterolateral border of the incisive foramen is formed by the median process of the maxilla, which is much thicker than the medial process and borders the posterior third of the lateral edge of the incisive foramen. The posterior extension of the incisive foramen up to the posterior edge of the canine as observed in MHNC 13906 is absent in the other Tiupampa metatherians (e.g., *Andinodelphys*, *Pucadelphys*, *Mayulestes*) and in the extant didelphids.

The left palatal process is less damaged than the right one. No palatal vacuity is observed but, at the level of the posterior edge of M2, a large major palatine foramen is present. The anteroposterior position of the foramen is similar to that observed in *Andinodelphys* and *Pucadelphys*. The major palatine foramen transmits the major palatine artery and nerve to the ventral region of the secondary palate. On the posterolateral region of the palate, the maxilla meets the minor palatine foramen.

Lacrimal (Figs 8; 9). The lacrimal is relatively large. It forms the anterior edge of the orbit, although it is mainly internal to it. The facial process is crescent-like and narrow. It does not strongly extend on the face as it does in the basal metatherians, deltatheroidans and sparassodonts (including *Mayulestes*). It resembles the condition in *Pucadelphys* and extant didelphids. The internal portion of the lacrimal is three to four times larger than the facial process. As discussed above, the lacrimal has a long suture with the maxilla anteriorly, a small suture with the nasal dorsally with the frontal posterodorsally, with the palatine posteroventrally and ventrally, and a small one with the jugal ventrolaterally. On the anterior edge of the orbit, but internal to it, two lacrimal foramina open posteriorly. They are subequal in size and roughly circular to oval-shaped. They are positioned one almost lateral to the other along a subhorizontal (dorsomedial-ventrolateral) axis; in other words, the lateral lacrimal foramen is slightly ventrolateral to the medial one. No lacrimal tubercle is observed. A lacrimal tubercle is absent in *Pucadelphys* and *Mayulestes*. It is present *Andinodelphys* and variably present in some extant didelphids (e.g., *Caluromys*, *Thylamys* – personal observations). Within the orbit, the lacrimal forms the dorsal edge of the maxillary foramen.

Nasal (Figs 8; 9). The nasals are elongated narrow bones, with sub-parallel edges in their anterior two thirds and which strongly widen in their posterior third. The anterior apices of the nasals are probably missing and it is not possible to observe if their anterior ends overhang the nasal fossa or not. The nasal-maxilla suture is anteroposteriorly oriented up to the level of P3. There, it turns laterally at approximately 45° and turns posteriorly just before contacting the lacrimal. Posterior to this bone, the nasal contacts the frontal and the nasal-frontal suture turns medially at approximately 45°. At the medial third of the frontal width, the suture turns antero-medially at 90° and meets the sagittal plane. The posterior suture of the nasals, with the frontals, is distinctly W-shaped as in *Pucadelphys* and in most didelphids (e.g., *Hyladelphys*, *Marmosa*, *Monodelphis*, *Metachirus*, *Didelphis*, *Lutreolina*, *Cryptomanus*, *Lestodelphys*, *Thylamys*). It differs from that of *Andinodelphys* in which it is markedly convex posteriorly. This posterior flared portion of the nasals is longer than wide, but not as elongated as in extant didelphids. It differs from the diamond-shaped morphology observed in *Andinodelphys*.

In its lateralmost region, the nasal contacts the lacrimal as is observed in sparassodonts and deltatheroidans. Posteriorly, the nasals extend approximately as far as mid-length of the orbit and remain well anterior to the supraorbital processes.

Jugal (Figs 8; 9). The jugals are preserved only in their anterior part, which articulates with the maxilla and which borders the orbit ventrolaterally. On its lateral aspect, in didelphids, this region of the jugal bears a deep elongated fossa for the origin of the *zygomaticus* and *levator labii superioris*. No fossa is observed in this region of the jugal of *Incadelphys*. The *levator labii superioris* probably originated in the fossa in the maxilla below the maxilla-jugal suture, as discussed above, and the *zygomaticus* probably originated on the jugal as in *Didelphis*,

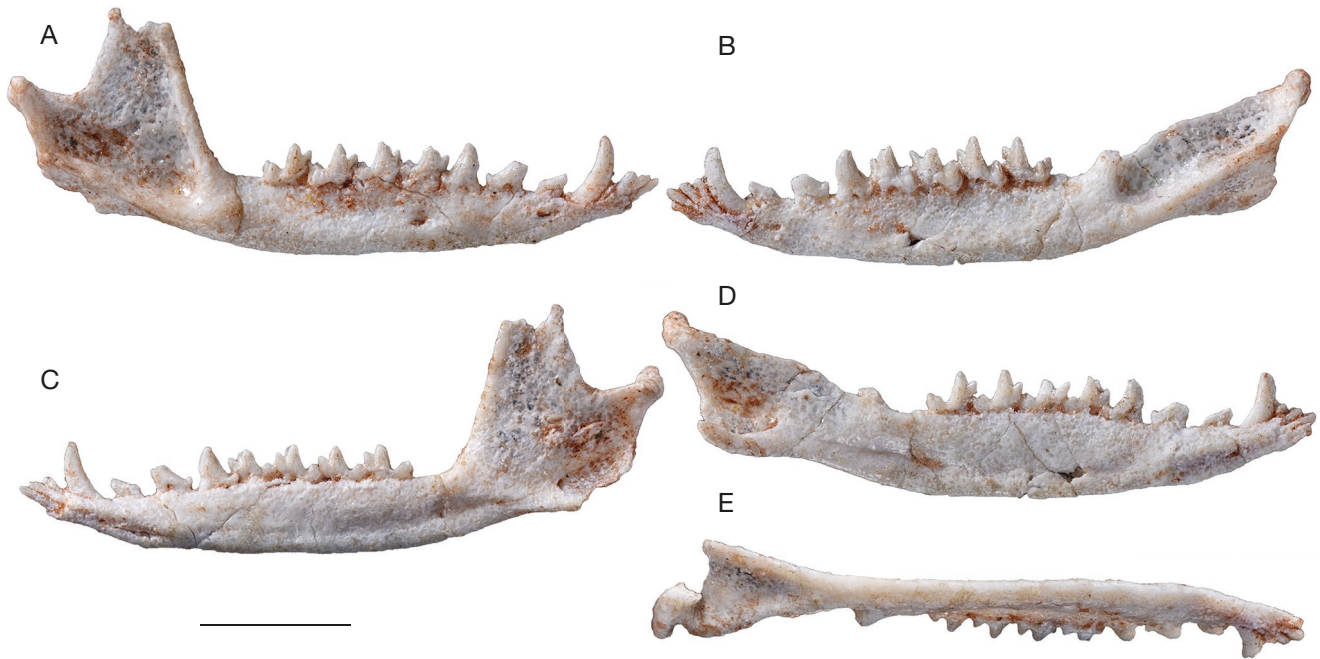


FIG. 10. — *Incadelphys antiquus*, MHNC 13906: **A**, lateral view of the right dentary; **B**, medial view of the right dentary; **C**, lateral view of the left dentary; **D**, medial view of the left dentary; **E**, ventral view of the left dentary. Scale bar: 5 mm.

although no fossa for this muscle is observed on the jugal of *Incadelphys*. The condition of the latter is similar to those of *Andinodelphys* and *Pucadelphys* and therefore clearly differs from that in extant didelphids.

Frontal (Figs 8; 9). Dorsally, a small part of the frontals is preserved, which forms the interorbital bridge. Anteriorly, the frontals feature conspicuous anterior processes which wedge between the nasals anteriorly. Laterally, the frontal bears a small and sharp supraorbital process as in *Andinodelphys* and *Pucadelphys*. Anteroventral to the process is a small anteriorly-opening frontal diploic foramen (Figs 8; 9). This foramen likely conveyed the frontal diploic vein, an emissary of the dorsal cerebral vein/dorsal sagittal sinus or a vein issued from the frontal diploe (Thewissen 1989; Evans & de Lahunta 2013; Wible *et al.* 2004). This foramen is called supraorbital foramen by Novacek (1986) and Marshall & Muizon (1995), the frontal foramen by Evans & de Lahunta (2013), the foramen for the frontal diploic vein by Wible & Rougier (2000), Wible (2003), Wible *et al.* (2009) and Wible (2011), and the frontal diploic foramen by Thewissen (1989). In this paper, we retain the terminology “frontal diploic foramen”. Such a foramen is present in *Pucadelphys*, *Andinodelphys*, and generally in Recent didelphids.

Dentary (Fig. 10). The dentary of *Incadelphys* is very slender and gracile to a greater extent than all the Tiupampa metatherians for which a complete dentary is known (Table 4). The dentary of *Incadelphys* is proportionally even longer and lower than in *Andinodelphys*, which has a notably elongated snout (Muizon & Ladevèze 2020). As seen in Table 4, the dentaries of *Pucadelphys* and *Mizquedelphys* are consistently shorter

proportionally than those of *Incadelphys* and *Andinodelphys* and the stouter metatherian dentaries known at Tiupampa are those of *Mayulestes* and *Allqokirus*. Therefore, a gradient of rostrum slenderness is observed in the Tiupampa metatherians increasing from the slenderest morphology in *Incadelphys* to the stouter in *Allqokirus-Mayulestes*: *Incadelphys* < *Andinodelphys* < *Pucadelphys* < *Mizquedelphys* < *Allqokirus-Mayulestes*.

The corpus mandibularis slightly increases in depth posteriorly and has a maximum elevation below m2-m3. Then it slightly decreases posteriorly as far as the retromolar space. The ventral edge of the corpus is weakly convex, the convexity being maximum below m4. It is less convex than in the extant didelphids *Didelphis* and *Caluromys*, in which the corpus is generally deeper, with the deepest point located more posteriorly, below m3-m4. The condition of *Incadelphys* more closely resembles, in this respect, that of *Andinodelphys*. Three mental foramina are observed, a small one below i3 and, on the lateral aspect of the corpus, two large mental foramina are present, the anterior one below p1 and the posterior one below m1. The foramen observed in *Andinodelphys* between the dorsal edge of the symphysis and the lingual alveolar border of the canine is absent in *Incadelphys*. On the medial aspect of the corpus, the mandibular symphysis is unfused. It is elongated and low and extends posteriorly as far as a point below the anterior root of p2. The long axis of the symphysis is at an angle of approximately 19° to the horizontal axis of the tooth row (the alveolar border), which resembles the condition in *Andinodelphys* (Muizon & Ladevèze 2020). As in this latter genus, the condition of *Incadelphys* is related to the anterior tapering of the rostrum and procumbency of the incisors. It contrasts with the shorter rostrum of *Pucadelphys*

TABLE 4. — Proportions of the dentary in Tiupampa metatherians and some didelphids. Abbreviations: **Hm3**, labial height of the dentary below m3 between trigonid and talonid; **L**, length of the dentary from the posterior edge of the condyle to the anterior end of the symphysis. Measurements for *Pucadelphys* and *Mayulestes* have been taken from Muizon *et al.* (2018: 415, table 5). Length of the dentary for *Allqokirus* is an estimation (e) of the adult length as evaluated by Muizon *et al.* (2018: 414) for the sub adult specimen MHNC 8267. Measurement are in mm.

	LD	Hm3	Hm3/ LD	Mean
<i>Incadelphys antiquus</i>				
MHNC 13906 (right)	21	2.30	0.109	
MHNC 13906 (left)	21.1	2.35	0.111	
Mean				0.110
<i>Andinodelphys cochabambensis</i>				
MHNC 8264	38.61	4.85	0.125	
MHNC 8308	39.10	4.65	0.119	
MHNC 8370	34.77	4.25	0.122	
Mean				0.122
<i>Pucadelphys andinus</i>				
MHNC 8266	25.90	3.49	0.134	
MHNC 8378	22.50	2.99	0.132	
MHNC 8380	21.68	2.89	0.133	
MHNC 8381	25.74	3.55	0.137	
MHNC 8382	26.33	3.61	0.137	
Mean				0.135
<i>Mizquedelphys pilpinensis</i>				
MHNC 13917(right)	18.7	2.80	0.149	
MHNC 8389 (left)	19.07	2.88	0.151	
Mean				0.150
<i>Mayulestes ferox</i> MHNC 1249	41.96e	6.40	0.152	0.152
<i>Allqokirus australis</i> MHNC 8267	32.98e	4.97	0.150	0.150
<i>Monodelphis brevicaudata</i>				
MNHN Zo-2003 762	29.19	3.68	0.126	
<i>Monodelphis brevicaudata</i>	31.4	3.7	0.118	
MNHN 2004-317				
<i>Monodelphis domestica</i>	28.96	3.33	0.115	
MNHN 1967-330				
<i>Monodelphis brevicaudata</i>	27.12	3.50	0.128	
MNHN 1995-3216				
Mean <i>Monodelphis</i> spp.				0.122
<i>Didelphis marsupialis</i>				
1900-581	85.27	14.5	0.170	
2007-8	83.1	13.1	0.157	
1932-3003	79.46	10.8	0.136	
2007-7	95.68	14.1	0.147	
Mean				0.152
<i>Philander opossum</i>				
2012-21	69.97	9.42	0.134	
1986-485	60.95	8.56	0.140	
2000-215	58.8	8.92	0.150	
1998-2264	58.83	7.63	0.130	
Mean				0.138

(c. 22.4°) and especially of *Mayulestes* (29°) and *Allqokirus* (30°) (see Muizon & Ladevèze 2020: table 7). Among extant didelphids, the condition of *Incadelphys* resembles that of *Metachirus*, but differs from *Didelphis* and *Caluromys*, in which the symphysis is slightly less slanted.

A conspicuous mylohyoid groove is present and extends from a point below p3 as far as a point below the anterior end of the coronoid crest. Between the last molar and the base of the coronoid crest is a small retromolar space, which is slightly shorter than m4.

On the ramus, the coronoid process is large but proportionally smaller than in *Didelphis*, shorter (proximodistally) than in *Caluromys*, and approaches the size observed in *Metachirus*. Its apex is incomplete but little of the process is missing. Because its posterior edge is straight it is probable that its apex was not (or little) recurved posteriorly, as is observed in *Andinodelphys* and *Pucadelphys*. The straight posterior border of the coronoid process differs from the condition generally observed in didelphids, but resembles the straight posterior border of the coronoid process in *Dasyurus*. The coronoid crest, which forms the anterior edge of the process, is straight and proportionally thinner than the condition observed in *Andinodelphys*, in which it is salient towards its base and extends on the lateral aspect of the body. The condition of *Incadelphys* resembles that of *Pucadelphys* in this respect. The masseteric fossa is remarkably deep, especially posteroventrally, in the region anteroventral to the condyloid process, and anteroventrally, posterior to the coronoid crest. In the posteroventral region of the masseteric fossa, a sub-horizontal posterior shelf fossa projects laterally, being distinctly convex. The maximum lateral extension of this shelf is just ventral to the anteriormost point of the anterior edge of the condylar process, being more posterior than in *Andinodelphys*. The medial surface of the coronoid process is smooth and flat to slightly convex medially and bears no anterior crest.

Ventrally, the posterior crest of the coronoid process turns posteriorly and joins the articular condyle. This crest descends more ventrally than the condyle before reaching it and form a distinct notch between the two processes (Fig. 10). It reaches the condylar process in its medial third and is approximately posterior to the m4 in the axis of the tooth row. Therefore, the lateral two thirds of the condyle are lateral to the tooth row and overhang the posteroventral region of the masseteric fossa. The condition of *Incadelphys* is similar to that observed in *Pucadelphys* and *Andinodelphys*. Only one third of the transverse length of the condyle is medial to the tooth row. The condyle is strongly elongated transversely and cylindrical. Its articular surface is posterodorsally oriented. In its medial portion the condyle tappers being anteroposteriorly shorter. The lateral part of the condyle is buttressed by the ascending posterior end of the posterior shelf of the masseteric fossa.

On the posteromedial edge of the condylar process, just ventral to the point of junction between the coronoid and condylar processes, a robust ridge descends towards the posteromedial edge of the angular process. In lateral view, the articular surface of the condyle is located above the apex of the protoconid of m4, at a distance of approximately twice the height of the trigonid of m4. Therefore, the condyloid process is in a much higher (c. four times more elevated) position than in *Andinodelphys* and *Pucadelphys*, in which the distance is approximately the height of the talonid of m4.

The angular process is shelf-like and inflected medially, as in most metatherians (Fig. 11E). It is triangular in ventral view and approximately twice as long as wide posteriorly. Its posterior edge is slightly concave, and its medial angle forms a short but pointed triangular process more pronounced than in *Pucadelphys* and *Andinodelphys* but clearly differ-

ing from the sharp, posteriorly-projecting spur-like process observed in didelphids and, to a greater extent, in dasyurids. In *Didelphis*, the dorsal surface of the angular process receives the insertion of the internal pterygoid and its ventral aspect supports the superficial masseter (Hiimeae & Jenkins 1969). Sanchez-Villagra & Smith (1997) have established categories of the diversity of the angular process in marsupials based on the ratio of “angular process length to angular process shelf length”. The ratio value calculated for *Incadelphys* is *c.* 0.83, which places it in the “shelf-like” category (Ratio > 0.81). However, it is noteworthy that this ratio is significantly lower than in *Andinodelphys* in which the ratio is 0.89. Therefore, the ratio calculated for *Incadelphys* reflects the length of the posteromedial process of the angular process, conspicuously longer than in *Andinodelphys*. Slightly posterior to the point of departure of the angular process, on its lateral side, is a small mandibular foramen. It is circular to oval-shaped and widens posteriorly. It is located ventral to the middle of the apex of the coronoid process.

DISCUSSION

COMPARISONS

Among the other Tiupampa metatherians, *Incadelphys* has been compared with *Mizquedelphys* by Marshall & Muizon (1988) and by Muizon (1992), who observed close similarities in terms of size and upper molar morphology. However, several partial skulls and mandibles of *M. pilpinensis* discovered since that time (currently under study by the authors) and the very complete new specimens of *I. antiquus* described here allow a more thorough comparison. All the new specimens of *I. antiquus* are characterized by an extreme slenderness of the cheek teeth (especially the uppers). In contrast, the robust cheek teeth of *M. pilpinensis* clearly resemble those of *Pucadelphys*, although much smaller. The upper premolars of *Incadelphys* are extremely compressed transversely, whereas those of *Mizquedelphys* are massive and its P3 even features a conspicuous distolingual accessory cusp, which is absent in the other pucadelphyids (i.e. *Pucadelphys* and *Andinodelphys*). The transverse compression observed on the upper premolars of *Incadelphys* is also present on the M1, in which the anterior styler shelf is almost absent, with the paracone greatly approximated to styler cusp B and a preparacrista much shorter than in *Mizquedelphys*. It is noteworthy that on the dP3 of the holotype of *I. antiquus* the paracone and styler cusp B are fused and the anterior styler shelf is lacking. The styler shelf of the other molars are similar in width in the two genera but it is deeper in *Incadelphys*. Except the features discussed above the molars of the two genera have a similar basic pattern differing only in the styler cusp C being more developed in *Mizquedelphys*, the entoconid being more developed (as high as or higher than the hypoconid) in *Incadelphys*, and the ectoflexus of M2-3, being slightly deeper in *Incadelphys*. Furthermore, *Mizquedelphys* lacks the characteristic distolabial extension of the metastyler angle of M1. However, the major difference between the two taxa is in the rostrum and

mandible length. As highlighted in Table 4, the proportions of the mandible (height below m3/total length of the dentary) of *Mizquedelphys* indicate a short and relatively massive rostrum, which more resembles the condition observed in the Tiupampa sparassodonts. In contrast, *Incadelphys* features the most elongated and slender rostrum among the Tiupampa metatherians for which a complete dentary is known (i.e. from condyle to incisors alveoli). Therefore, it is clear that the external morphology of the head was significantly different in *Incadelphys* and *Mizquedelphys* even if the two taxa were approximately of the same size.

Among the other metatherians of Tiupampa, *Incadelphys antiquus* also compares favorably with *Szalinia gracilis*, although the former is significantly larger (Muizon & Cifelli 2001). In general morphology, the teeth of *Szalinia* are more gracile than those of *Incadelphys* except the upper premolars which are transversely wider and relatively more robust, with a well-developed cuspule at the mesial base of P3 (absent in *Incadelphys*). The upper molars of *Szalinia* are transversely wider and mesiodistally shorter than those of *Incadelphys*. *Szalinia* also differs from *Incadelphys* in the extreme development of the parastylar lobe of the upper molars (especially M3-M4), in which the styler cusps A and B are connate or fused, a condition that is absent in *Incadelphys*. The upper molars of *Szalinia* also differ from those of *Incadelphys* in the wider anterior styler shelf of M1-M3, the protocone being transverse (shifted mesially in *Incadelphys*) and less compressed mesiodistally, in the larger styler cusp C, and in the absence of a distolabial extension of metastyler angle of M1. The lower premolars and molars of *Szalinia* are more robust than those of *Incadelphys*, being proportionally shorter and wider with a vertical distal edge of trigonid (sloping in *Incadelphys*). Diastemata between the premolars are absent or more reduced in *Szalinia*. Diastemata are lacking between the upper premolars and between P3 and M1; they are absent between p3 and p2 and shorter than in *Incadelphys* between p2 and p1. Therefore, the dental morphology and implantation of *Szalinia* indicate a proportionally shorter cheek tooth row than in *Incadelphys*. This is confirmed by the much shorter retromolar space and the subvertical (sloping in *Incadelphys*) anterior edge of the coronoid process in *Szalinia*.

Marshall & Muizon (1988) and Muizon (1992) have mentioned that, among the metatherians of the early Eocene of Itaboraí, *Incadelphys antiquus* is remarkably similar to, and compare best with, *Marmosopsis juradoi*. However, it differs from the latter in the deeper styler shelf basin, the dorsoventrally concave postmetacrista (straight in *Marmosopsis*), the larger protocone (corresponding to a larger talonid), the wider crowns of lower molars, the trigonid slightly more inclined anteriorly (more vertical in *Marmosopsis*), the larger paraconid (as compared to the metaconid), the higher metaconid as high as the protoconid, (lower in *Marmosopsis*), the entoconid higher than the hypoconid (lower in *Marmosopsis*), the slightly longer talonid, the much larger talonid of m4 (talonid of m4 distinctly reduced in *Marmosopsis*), and the pre- and post-cingulids more developed. However, these differences being minor, these authors regarded *Incadelphys*

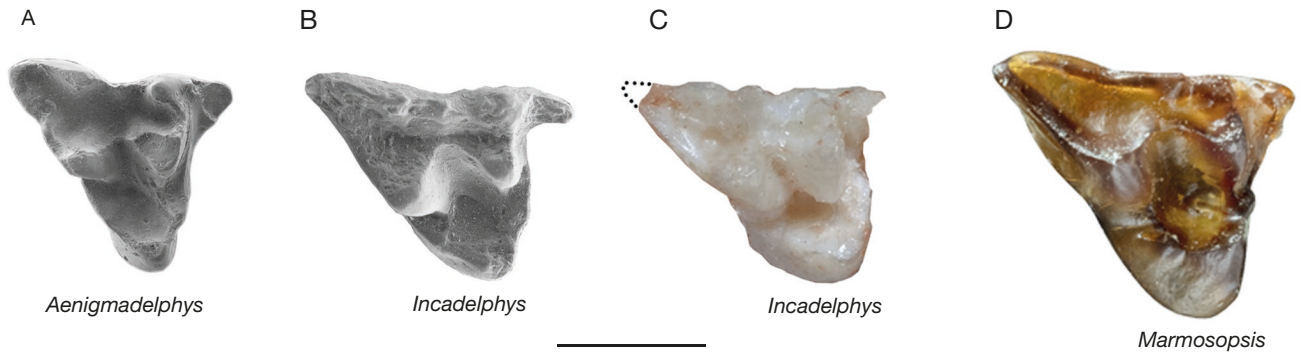


FIG. 11. — Occlusal view of the M1 of some basal metatherians discussed in text showing the distolabial extension of the metastylar lobe: **A**, *Aenigmadelphys* (OMNH 22898), SEM photo of cast; **B**, *Incadelphys* (YFPB Pal 6251), SEM photo of cast; **C**, *Incadelphys* (MHNC 13906); **D**, *Marmosopsis* (MNHN.F.ITB83). Scale bar: 1 mm.

as a potential morphological ancestor for *Marmosopsis*. The comparison provided above (Table 3) of the metastylar angle of M1 in both taxa reinforces this statement. This interpretation is followed here.

The above diagnosis and description have also revealed consistent resemblances between *Incadelphys* and *Aenigmadelphys* from the Campanian of Utah (Fig. 11; 12). One of the major characteristics shared by the two genera is the strong distolabial extension of the metastylar angle of M1 (Table 3). The angle between the line joining stylar cusp D and E and the postmetacrista (36° in *Incadelphys* and 40° in *Aenigmadelphys*) is clearly smaller than in the other Tiupampa metatherians (51.4° in *Pucadelphys* and 58.3° in *Andinodelphys*, 50° in *Mizquedelphys*). The angle in *Incadelphys* and *Aenigmadelphys* is also close to that measured in four specimens of *Marmosopsis* from the early Eocene of Itaboraí (mean = 39°).

Besides the extension of the metastylar angle, *Incadelphys antiquus* and *Aenigmadelphys archeri* resemble each other in the following combination of features:

- 1) the flat to concave labial edges of the para- and metacone, with labial displacement of the centrocrista and very slightly V-shaped centrocrista (i.e. para- and metacone are triangular in cross-section);
- 2) preparacrista running anterior to, rather than joining, stylar cusp B;
- 3) postmetacrista distinctly concave dorsoventrally in posterior view;
- 4) stylar cusp C very small and much smaller than B and D;
- 5) stylar cusp D distinctly smaller than B on M2-M3;
- 6) postmetaconular crista does not extend below metacone up to stylar cusp E but extends somewhat on mesiolingual region of metacone;
- 7) trigonid and talonid subequal in width on m2-m3;
- 8) posterior edge of metaconid sloping and trigonid slightly inclined anteriorly;
- 9) paraconid placed lingually and in line with metaconid and entoconid;
- and 10) entoconid higher than hypoconid.

Nevertheless, although notable similarities exist between the two species, *Incadelphys antiquus* differs from *Aenigmadelphys archeri* in the following features:

- 1) paracone smaller than metacone (larger in *Aenigmadelphys*);
- 2) protocone mesiodistally shorter labially;
- 3) anterior stylar shelf slightly (strongly on M1) narrower than posterior (subequal in width in *Aenigmadelphys*);
- 4) stylar shelf on M2-3 slightly narrower;
- 5) ectoflexus absent on M1 (present but small in *Aenigmadelphys*);
- 6) metaconid larger as compared to paraconid on m2-m3 (almost subequal in size in *Aenigmadelphys*);
- 7) paracristid straight with paraconid in a more anterior position (paracristid convex anteriorly with paraconid more posteriorly placed in *Aenigmadelphys*);
- and 8) metaconid almost as high as protoconid (distinctly lower in *Aenigmadelphys*).

These differences are minor and considering the age difference between the two taxa *Aenigmadelphys* indeed displays a morphology close to that of a potential ancestral morphotype for *Incadelphys*. Among the North American Late Cretaceous, the dental anatomy of *Aenigmadelphys* is very peculiar and does not resemble that of any other Late Cretaceous North American taxa; this is especially true concerning the triangular cross-section of the para- and metacone and the distolabial extension of the metastylar area of M1. The only genera that resemble *Aenigmadelphys* for these two characters are *Incadelphys* and *Marmosopsis* as expressed above.

The major difference between *Aenigmadelphys* and *Incadelphys* is the relative size of para- and metacone. However, it is noteworthy that a paracone larger or subequal to metacone is present in all the Late Cretaceous North American metatherians (except in stagodontids, some pediomyids, and *Glasbius*) and likely represents a plesiomorphy (Cifelli & Johanson 1994). In contrast, the paracone is smaller than the metacone in all the South American metatherians except *Peradectes austrinum* (from Laguna Umayo, Peru) and *P. cf. austrinum* (from Tiupampa, Bolivia), in which the cusps are subequal (as in most peradectids). It is worth noting that in highly derived South American taxa (e.g., most Paucituberculata or Polydolopimorphia), either the para- and metacone are subequal in size or the molar modification is so extreme that such a size comparison is meaningless. Nevertheless, the paracone is distinctly smaller than the metacone in *Roberthoffstetteria*,

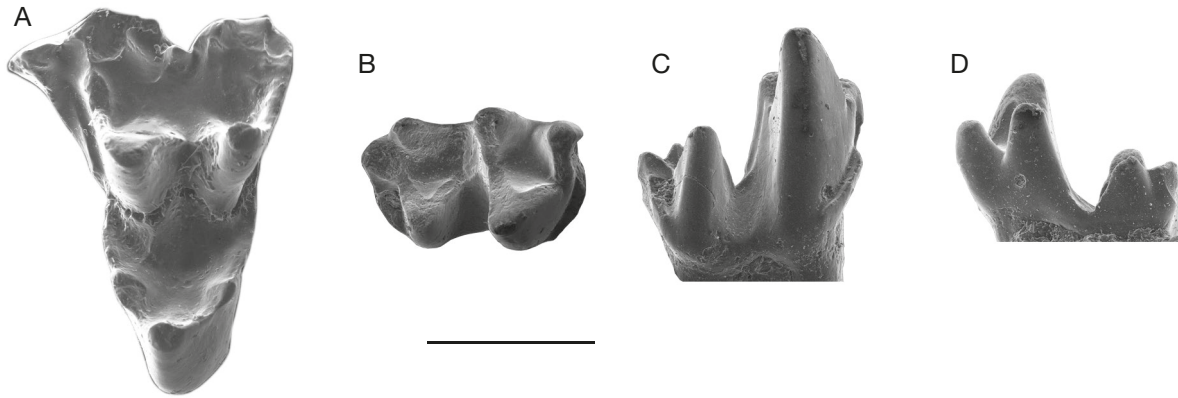


FIG. 12. — *Aenigmadelphys archeri*, SEM photos of casts: **A**, left M3 (holotype, OMNH 23328) in occlusal view; **B**, right m3 (OMNH 20531) in occlusal view; **C**, the same in labial view; **D**, the same in lingual view. Scale bar: 1 mm.

which is the most plesiomorphic polydolopimorphian (Goin *et al.* 2003), and in *Perulestes*, the oldest known caenolestoid (Goin & Candela 2004). This relative size of the paracone and metacone observed in the oldest representative of these orders indicates that it also represents the plesiomorphic condition for these highly specialized South American metatherians.

RESULTS OF THE PHYLOGENETIC ANALYSIS

A first analysis was performed with unweighted characters. The analysis resulted in four shortest trees (Tree length [L] = 884; Consistency index [CI] = 0.402; Retention index [RI] = 0.610). The strict consensus is represented in Figure 13 (L = 889; CI = 0.4; RI = 0.606). It clearly indicates a close relationship of *Incadelphys* with *Marmosopsis*, *Aenigmadelphys* and *Szalinia* although the four taxa do not form a clade, but are a paraphyletic assemblage stem to Sparassodonta. In the following discussion, these four taxa whether they constitute a paraphyletic or monophyletic grouping will be designated as the SAMI group, from the initials of the four genera. It is noteworthy that the paraphyletic relationships of the SAMI retrieved in the unweighted analysis are poorly supported as indicated by the low Bremer indices on Figure 13. Furthermore, as retrieved by Muizon & Ladevèze (2020), *Itaboraidelphys* is confirmed as the sister group to *Andinodelphys* and *Pucadelphys*, the three taxa constituting the Pucadelphyidae, which are grouped with the Sparassodonta within the clade Pucadelphyda defined by Muizon *et al.* (2018), in which are now included *Incadelphys*, *Szalinia*, *Marmosopsis* and *Aenigmadelphys*. The relationships of *Itaboraidelphys* to *Andinodelphys* and *Pucadelphys* differs from that retrieved by Oliveira *et al.* (2016) and Rangel *et al.* (2019). These authors, included *Itaboraidelphys* in the Notometatheria as the sister taxon of *Didelphopsis*. In fact, this difference is most likely related to our hypothesis to refer the two Type II Itaboraí petrosals to *Itaboraidelphys* (following Muizon *et al.* [2018]), what Rangel *et al.* (2019) did not (see also Muizon & Ladevèze 2020).

In a matrix based on morphology, the proportion of homoplastic characters is likely to be large, and when so the homologous phylogenetic signal is difficult to be discriminated from homoplasy and it may product erroneous topologies (e.g.,

Murphy *et al.* 2021). As a matter of fact, our strict consensus tree is framed by weakly supported branches (weak Bremer indices, most of the deepest nodes being inferior or equal to 2), and an alternate hypothesis with an overweighting of the least homoplastic characters needs to be considered. These are the reasons why we decided to constraint our analysis with a strong control of homoplasy, with a second analysis using imply weighting. As discussed above we do not use a constant with higher values (as recommended by Goloboff *et al.* 2017) because such values retrieved consensus trees almost identical to the strict consensus (with no incidence on the South American taxa) and did not downweight enough homoplastic characters. With a k-value of 3 (as previously recommended by Goloboff 1993), the implied weighting analysis resulted in two shortest trees with the following scores: CI = 0.401; RI = 0.609. In the strict consensus (CI = 0.4; RI = 0.606), the relationships of the Didelphidae included in the analysis are not fully resolved (Fig. 14). In contrast, the relationships of *Incadelphys* with *Marmosopsis*, *Aenigmadelphys* and *Szalinia* are more consistent with the notable similarities observed in the comparison above, especially between the first three former taxa and the SAMI is now a clade, a topology which we favor here as compared to that resulting from the unweighted analysis (Fig. 13). *Incadelphys* is sister to *Marmosopsis*, and both form a clade with *Aenigmadelphys*. *Szalinia* is sister taxon to this clade. A sister group relationship of *Incadelphys* and *Marmosopsis* within a clade including *Szalinia* has already been retrieved by Carneiro *et al.* (2018), who also included within this clade the other Tiupampan genera *Jaskhadelphys* and *Tiulordia*, as well as other Brazilian and Peruvian taxa. We have mentioned above (material and method section) the reasons why we did not include *Jaskhadelphys* and *Tiulordia* in our analysis. We rather not formally designate the SAMI clade because, if a potential discovery of new material of *Jaskhadelphys* allows to securely include this taxon in the SAMI clade, then it should be named Jaskhadelphyidae, which was created by Muizon (1992). However, as mentioned above, we regard the current phylogenetic affinities of *Jaskhadelphys* retrieved by others (Oliveira *et al.* 2016; Carneiro 2018; Carneiro *et al.*

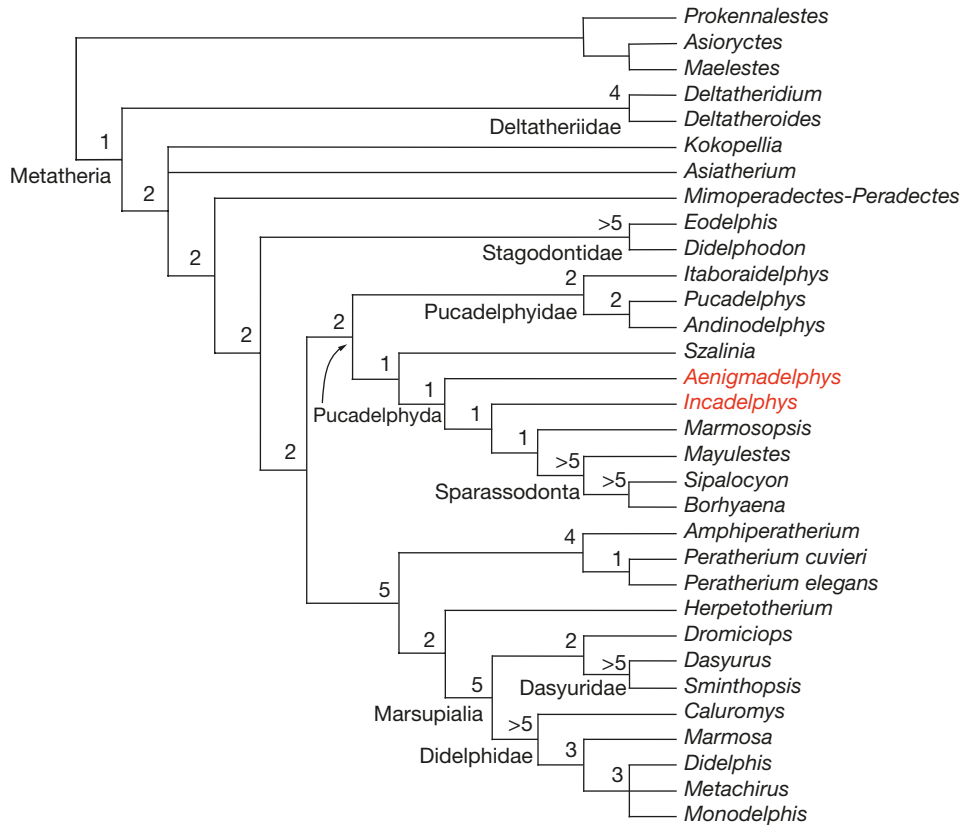


FIG. 13. — Phylogenetic relationships of *Incadelphys* among other metatherians: strict consensus tree of four equally parsimonious trees resulting from the analysis of the data matrix of 287 osteological characters and 32 taxa with equally weighted homoplastic characters (Tree length [L] = 889; Consistency index [CI] = 0.4; Retention index [RI] = 0.606); the Bremer index is given at branches in black numbers below nodes.

2018; Rangel *et al.* 2019) as poorly established in regard of the extreme scarcity of the material available so far. In our implied weighting analysis, the SAMI forms a clade, sister to Pucadelphyidae. An alternative would therefore be to include the SAMI within the latter. However, because the SAMI is not monophyletic in the unweighted analysis, we rather retain this grouping unnamed even if, in both analyses, it is clearly included in Pucadelphyda.

The clade Pucadelphyidae + SAMI is supported by three unambiguous synapomorphies:

- 37 (1) Paracone slightly smaller than metacone (see Appendix 1) [reversal from clade (stagodontids ((Pucadelphyda) (herpetotheriids (Marsupialia)))); convergent with *Dromiciops*; subequal or slightly larger in *Aenigmadelphys*];
- 105 (2) Postorbital process conspicuous and protruding (convergent with peradectids);
- 114 (0) Medial and lateral palatal processes of the maxilla approximately of the same size.

Pucadelphyidae + SAMI may also be supported by 18 ambiguous synapomorphies (Acctran, fast):

- 16 (1) Diastema posterior to P1 present [convergent with *Asiatherium*, *Sipalocyon*, and (*Herpetotherium*, Marsupialia); reversal in *Szalinia*];

- 29 (0) Postmetacrista on antepenultimate or penultimate molars subequal to shorter than preparacrista [reversal from clade (stagodontids ((Pucadelphyda) (herpetotheriids (Marsupialia)))); reversal in (*Marmosopsis*, *Incadelphys*); convergent with (*Herpetotherium*, Marsupialia)];
- 54 (0) Trigonid wider than long [reversal from clade ((Pucadelphyda) (herpetotheriids (Marsupialia)))); convergent with *Sminthopsis*; longer than wide in *Marmosopsis*];
- 68 (0) Paracristid and protocristid subequal in length [reversal from clade ((Pucadelphyda) (herpetotheriids (Marsupialia))));
- 79 (0) Postcingulid on ultimate lower molar present [reversal from clade ((Pucadelphyda) (herpetotheriids (Marsupialia)))); reversal in *Pucadelphys*];
- 100 (0) Posterior end of the facial (posterodorsal) process of the premaxilla above canine or anterior [reversal from clade (stagodontids ((Pucadelphyda) (herpetotheriids (Marsupialia)))); convergent with (*Herpetotherium*, Marsupialia)];
- 130 (1) Sagittal crest restricted to parietals [reversal from clade (stagodontids ((Pucadelphyda) (herpetotheriids (Marsupialia))));
- 134 (0) Postglenoid process higher than wide and roughly parabolic [reversal from clade (peradectids (stagodontids ((Pucadelphyda) (herpetotheriids (Marsupialia)))); convergent with Marsupialia];

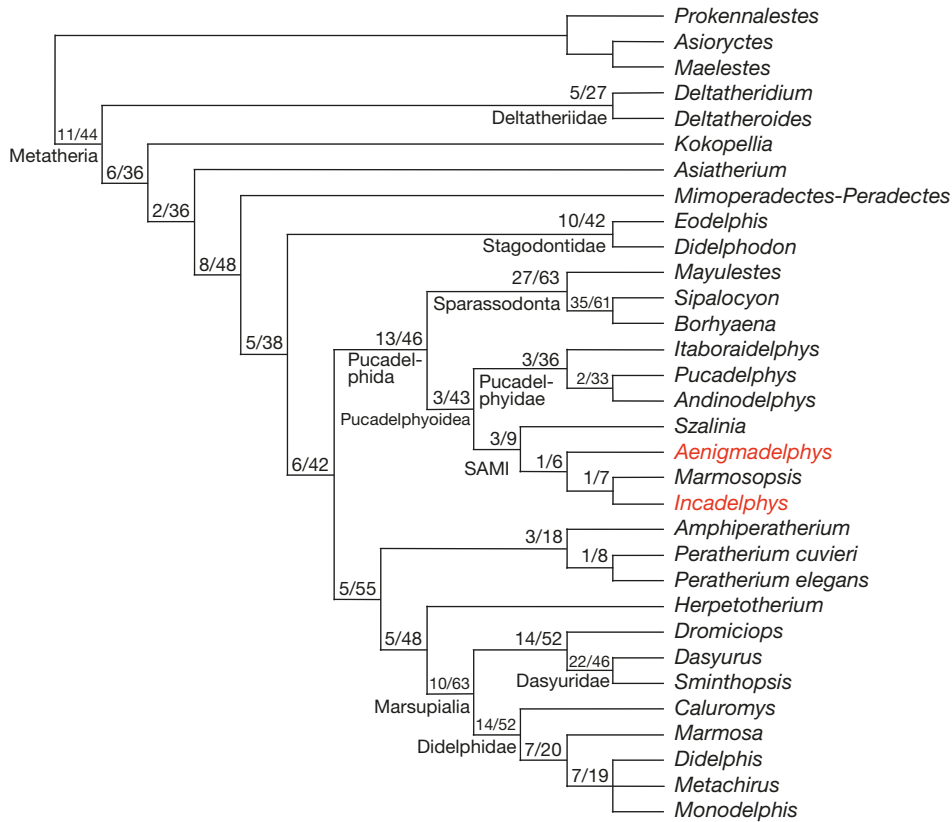


FIG. 14. — Phylogenetic relationships of *Incadelphys* among other metatherians: strict consensus tree (Consistency index [CI] = 0.401; Retention index [RI] = 0.609) of the two shortest trees resulting from the analysis with downweighted homoplastic characters (with Goloboff $k = 3$); black number above nodes indicate the minimum and maximum numbers of synapomorphies. The name of clade designated as “SAMI” is a working term composed with the initials of the four genera it includes: *Szalinia*, *Aenigmadelphys*, *Marmosopsis*, and *Incadelphys*.

- 171 (0) Stapedius fossa approximately twice the size of the fenestra vestibuli [reversal from Metatheria excluding deltatheriids; convergent with *Metachirus*, dasyurids, and (*Amphiperatherium*, *Peratherium*)];
- 191 (0) Ventral foramen on transverse process of the atlas, absent (reversal from Metatheria; convergent with dasyurids);
- 210 (0) Acromion process posterior to anterior edge of glenoid cavity (convergent with Didelphinae and *Dasyurus*);
- 230 (0) Distolateral process of Scaphoid absent [reversal from clade (peradectids (stagodontids ((Pucadelphyda) (herpetotheriids (Marsupialia)))))];
- 243 (1) Proximal width and length subequal (convergent with *Sminthopsis*);
- 244 (1) Tibia straight;
- 245 (1) No torsion between proximal and distal ends of tibia (convergent with Australidelphia);
- 251 (1) Medial plantar tuberosity of astragalus visible in dorsal view (convergent with *Eodelphis* and Marsupialia);
- 274 (1) Tuber calcis not curved ventrally (convergent with *Sipalocyon* and Marsupialia);
- 281 (1) MtII extends more proximally than Mt III (convergent with dasyurids).

Pucadelphyda + SAMI may also be supported by six ambiguous synapomorphies (Deltran, slow):

- 35 (0) Stylar cusp E present and distinct [reversal from clade (peradectids (stagodontids ((Pucadelphyda) (herpetotheriids (Marsupialia))))]; convergent with *Mayulestes*];
- 38 (1) Paracone and metacone triangular (flat labial face) [convergent with (herpetotheriids, Marsupialia)];
- 41 (1) V-shaped centrocrista [convergent with (herpetotheriids, Marsupialia)];
- 45 (1) Conules wing-like cristae absent [reversal from Metatheria excluding deltatheriids; convergent with *Sminthopsis* and (*Amphiperatherium*, *Peratherium*)];
- 81 (2) Angled ventral margin below last molar (convergent with *Didelphodon*, *Sipalocyon*, and dasyurids);
- 107 (1) External part of the lacrimal totally absent or reduced to a narrow crescentic rim on the anterior edge of the orbit (convergent with *Borhyaena*, Marsupialia, and *Peratherium*).

The SAMI clade is supported by three unambiguous synapomorphies:

- 52 (2) Trigonid basin anteroposteriorly compressed with cristids subparallel (reversal from Metatheria; convergent with stagodontids, *Pucadelphys*; reversal in *Marmosopsis*);

- 109 (1) Lacrimal foramen within the orbit (faces posteriorly) [convergent with (*Sipalocyon*, *Borhyaena*), and *Herpetotherium*];
- 118 (1) Posterior edge of the palate even with ultimate molar [reversal from clade (peradectids (stagodontids ((Pucadelphyda) (herpetotheriids (Marsupialia))))); convergent with (*Sipalocyon*, *Borhyaena*)].

The SAMI clade may also be supported by three ambiguous synapomorphies (Acctran, fast):

- 5 (0) I5 subequal to larger than I4 [convergent with (herpetotheriids, Marsupialia)];
- 13 (0) P1/p1 or P2/p2 parallel or subparallel to tooth row (reversal from Pucadelphyda, convergent with *Sipalocyon*);
- 75 (0) Entoconid at posterolingual angle of the tooth [reversal from clade (peradectids (stagodontids ((Pucadelphyda) (herpetotheriids (Marsupialia))))); convergent with stagodontids and (*Herpetotherium*, Marsupialia)].

The SAMI clade may also be supported by one ambiguous synapomorphy (Deltran, slow):

- 46 (0) Protocone small and anteroposteriorly narrow (reversal from Metatheria excluding deltatheriids; convergent with *Mayulestes* and *Sipalocyon*).

The AMI (Aenigmadelphys + Marmosopsis + Incadelphys) clade is supported by one unambiguous synapomorphy:

- 36 (1) Extreme posterolabial extension of metastylar angle of M1 present [convergent with Sparassodonta, Didelphinae, dasyurids, and (*Amphiperatherium*, *Peratherium*)].

The AMI clade is supported by one ambiguous synapomorphy (Acctran, fast):

- 18 (2) Blade-like premolars.

The sister group relationship of Incadelphys and Marmosopsis is supported by one unambiguous synapomorphy:

- 29 (1) Postmetacrista on antepenultimate molar or penultimate molar longer than preparacrista (reversal from node Pucadelphydae + SAMI; convergent with didelphids, *Dasyurus*, and *Deltatherium*).

The clade Incadelphys + Marmosopsis may also be supported by one ambiguous synapomorphy (Acctran, fast):

- 74 (0) Entoconid lower than hypoconid [reversal from Metatheria excluding deltatheriids; convergent with *Mayulestes* and (herpetotheriids, Marsupialia)].

The clade Incadelphys + Marmosopsis may also be supported by one ambiguous synapomorphy (Deltran, slow):

- 18 (2) Blade-like premolars [= ambiguous synapomorphy of AMI].

CONCLUSIONS

The results retrieved from the parsimony analyses performed in this study are in agreement with the conclusion of Marshall & Muizon (1988) and Muizon (1992), who regarded *Incadelphys* as closely related to *Marmosopsis*, but with a more plesiomorphic morphology. Close relationships of *Incadelphys* with *Marmosopsis* have also been brought to light by Oliveira *et al.* (2016) and Carneiro *et al.* (2018) as a result of the parsimony analyses performed by these authors. Our results therefore confirm the previous topologies retrieved by these authors, although we did not use the same data matrix. Furthermore, the phylogenetic affinities of *Szalinia* obtained in our two consensus trees also confirm the results of Rangel *et al.* (2019), who included this genus in Pucadelphyda; in our trees, as well as in Rangel *et al.* (2019), *Szalinia* is in a basal position of the clade in which it is included. However, the most interesting novelty resulting from our study is the relationships of *Aenigmadelphys* with the South American taxa included in our analysis, especially with pucadelphyids.

Such close affinities have been already suggested by Muizon & Ladevèze (2020: 694), who observed great similarities between pucadelphyids and *Aenigmadelphys* and stated that the latter could represent an ancestral North American morphotype for the South American pucadelphydan radiation. The close relationships retrieved in our analysis (with unweighted characters and with implied weighting $k = 3$) confirm this hypothesis. Moreover, it is noteworthy that *Szalinia* is more basal than *Aenigmadelphys* in both trees.

Aenigmadelphys is from the late Campanian of the Kaiparowits Formation of Utah and is approximately 10 Ma older than the Tiupampa fauna. Because no other metatherian from beds between the Kaiparowits Formation time and the end of the Cretaceous better resembles the pucadelphydians (in general) and *Incadelphys* (in particular), a large gap exists between *Aenigmadelphys* and its potential South American relatives. Nevertheless, it is noteworthy that a similar gap also exists between *Incadelphys* (early Danian) and *Marmosopsis* (early Ypresian).

It is noteworthy that our results are poorly supported at certain nodes (low Bremer indices) and must be taken cautiously, particularly regarding the SAMI taxa (a paraphyletic grouping in the strict consensus of the analysis with unweighted characters). Especially, the affinities of *Aenigmadelphys* with *Incadelphys* and *Marmosopsis*, which are based exclusively on dental characters, may be biased by the absence or scarcity of cranial characters for these taxa. To conclude, we believe that, if *Aenigmadelphys* represents, so far, the best North American “ancestral dental morphotype for Pucadelphyda”, its affinities to this superorder must be more firmly established and the discovery of cranial material of this genus is much needed to test the hypothesis presented here.

Be that as it may, the result of our analysis confirms the affinities of the Tiupampa mammal fauna, not only with the South American post-Palaeocene metatherian radiations but also with some Campano-Maastrichtian North American taxa, thus reinforcing its transitional condition between the Late Cretaceous Northern and Cenozoic Southern metatherian faunas.

Acknowledgements

The locality of Tiupampa was discovered in 1982 during a field expedition funded by National Geographic Society (grant N°2467/82). The specimen described in this paper has been discovered during a field season (2006) at Tiupampa, funded by the MNHN (Muséum national d'Histoire naturelle, Paris, France). Fossil collecting was carried out under the auspices of research agreements between the Museo de Historia Natural "Alcide d'Orbigny" de Cochabamba (MHNC), (Bolivia) and the Muséum National d'Histoire Naturelle. The specimens are the property of the MHNC and have been provided on loan to the MNHN for curation and study. Field expedition has benefited of logistical support from the IRD (Institut de Recherche pour le Développement) in Bolivia. We thank our Bolivian colleague Ricardo Céspedes-Paz for his collaboration and logistic support during the field season. Special thanks are due to Céline Bens, Aurélie Verguin, Géraldine Véron, and Christine Lefèvre, (MNHN), who provided access to MNHN specimens under their care. Warm thanks to Richard Cifelli for generously providing hundreds of casts of North American Cretaceous metatherians (including *Aenigmadelphys archeri*). Special thanks are due to the reviewers, Robin Beck, Francisco Goin, and Edison Oliveira whose invaluable comments significantly improved the manuscript. Photographs were made by Philippe Loubry and Lilian Cazes.

REFERENCES

- BREMER K. 1988. — The limits of amino acid sequence data in angiosperm phylogenetic reconstruction. *Evolution* 42 (4): 795-803. <https://doi.org/10.2307/2408870>
- CABRERA A. 1927. — Datos para el conocimiento de los dasyuroideos fósiles argentinos. *Revista del Museo de la Plata* 30: 271-315.
- CARNEIRO L. M. 2018. — A new species of *Varalphadon* (Mammalia, Metatheria, Sparassodonta) from the upper Cenomanian of southern Utah, North America: Phylogenetic and biogeographic insights. *Cretaceous Research* 84: 88-96. <https://doi.org/10.1016/j.cretres.2017.11.004>
- CARNEIRO L. M., OLIVEIRA E. V. & GOIN F. J. 2018. — *Austropedomyia marshalli* gen. et sp. nov., a new peditomyoidea (Mammalia, Metatheria) from the Paleogene of Brazil: Paleobiogeographic implications. *Revista Brasileira de Paleontologia* 21 (2): 120-131. <https://doi.org/10.4072/rbp.2018.2.03>
- CIFELLI R. L. 1993. — Early Cretaceous mammal from North America, and the evolution of marsupial dental characters. *Proceedings of the National Academy of Sciences* 90: 9413-9416. <https://doi.org/10.1073/pnas.90.20.9413>
- CIFELLI R. L. & JOHANSON Z. 1994. — New mammal from the upper Cretaceous of Utah. *Journal of Vertebrate Paleontology* 14 (2): 292-295. <https://doi.org/10.1073/pnas.90.20.9413>
- CIFELLI R. L. & MUIZON C. DE 1997. — Dentition and jaw of *Kokopellia juddi*, a primitive marsupial or near-marsupial from the Medial Cretaceous of Utah. *Journal of Mammalian Evolution* 4 (4): 241-258. <https://doi.org/10.1023/A:1027394430433>
- CIFELLI R. L. & MUIZON C. DE 1998. — Tooth eruption and replacement pattern in early marsupials. *Comptes Rendus de l'Académie des Sciences, Paris, Sciences de la Terre et des planètes* 326: 215-220. <https://doi.org/10.1017/S0022336000024306>
- CLEMENS W. A. 1966. — Fossil mammals from the type Lance Formation, Wyoming. Part II. Marsupialia. *University of California Publications in Geological Sciences* 62: 1-122.
- CLEMENS W. A. 1968. — A mandible of *Didelphodon vorax* (Marsupialia, Mammalia) *Contribution in Science* 133: 1-11. <https://doi.org/10.5962/p.241122>
- CROCHET J.-Y. 1980. — *Les marsupiaux du Tertiaire d'Europe*. Éditions de la Fondation Singer Polignac, Paris, 279 p.
- DAVIS B. M. 2007. — A revision of "pediomyid" marsupials from the Late Cretaceous of North America. *Acta Palaeontologica Polonica* 52: 217-256.
- EATON J. G. 1993. — Therian mammals of the Cenomanian (Late Cretaceous) Dakota Formation, southwestern Utah. *Journal of Vertebrate Paleontology* 13: 105-124. <https://doi.org/10.1080/02724634.1993.10011491>
- EVANS H. E. & DE LAHUNTA A. 2013. — *Miller's Anatomy of the Dog*. Saunders, St Louis, 850 p.
- FOX R. C. 1981. — Mammals from the Upper Cretaceous Oldman Formation, Alberta. V. *Eodelphis* Matthew, and the evolution of the Stagodontidae (Marsupialia). *Canadian Journal of Earth Sciences* 18 (2): 350-365. <https://doi.org/10.1139/e81-027>
- FOX R. C. 1983. — Notes on the North American Tertiary marsupials *Herpetotherium* and *Peradectes*. *Canadian Journal of Earth Sciences* 20 (10): 1565-1578. <https://doi.org/10.1139/E83-146>
- FOX R. C. & NAYLOR B. G. 1986. — A new species of *Didelphodon* Marsh (Marsupialia) from the Upper Cretaceous of Alberta, Canada: paleobiology and phylogeny. *Neues Jahrbuch für Geologie und Paläontologie* 172 (3): 357-380.
- FOX R. C. & NAYLOR B. G. 2006. — Stagodontid marsupials from the Late Cretaceous of Canada and their systematic and functional implications. *Acta Palaeontologica Polonica* 51(1): 13-36.
- GABBERT S. L. 1998. — Basicranial anatomy of *Herpetotherium* (Marsupialia: Didelphimorphia) from the Eocene of Wyoming. *American Museum Novitates* 3235: 1-13. <http://hdl.handle.net/2246/3244>
- GAYET M., MARSHALL L. G. & SEMPERE T. 1992. — The Mesozoic and Palaeocene vertebrates of Bolivia and their stratigraphic context: a review. *Revista Técnica de YPF* 12 (3-4): 393-433.
- GELFO J., GOIN F., WOODBURN M. O. & MUIZON C. DE 2009. — Biochronological relationships of South American Paleogene mammalian faunas. *Palaeontology* 52: 251-269. <https://doi.org/10.1111/j.1475-4983.2008.00835.x>
- GHEERBRANT E. 1992. — Les mammifères paléocènes du bassin d'Ouarzazate (Maroc). I. Introduction générale et Palaeoryctidae. *Palaeontographica* (A) 224: 67-132.
- GOIN F. J. & CANDELA A. 2004. — New Paleogene marsupials from the Amazon Basin of Eastern Peru, in CAMPBELL K. E. Jr (ed.), *The Paleogene Mammalian Fauna of Santa Rosa, Amazonian Peru*. Natural History of Los Angeles County, Los Angeles: 15-60 (Science Series; 40).
- GOIN F. J., CANDELA A. & MUIZON C. DE 2003. — The affinities of *Roberthoffstetteria nationalgeographica* (Marsupialia) and the origin of the polydolopine molar pattern. *Journal of Vertebrate Paleontology* 23: 869-876. <https://doi.org/10.1671/2383-11>
- GOIN F. J., WOODBURN M. O., ZIMICZ A. N., MARTIN G. M. & CHORNOGUBSKY L. 2016. — *A Brief History of South American Metatherians. Evolutionary Contexts and Intercontinental Dispersals*. Springer, Dordrecht, 237 p. <https://10.1007/978-94-017-7420-8>
- GOLOBOFF P. A. 1993. — NONA (a bastard son of Pee-Wee). Version 2.0. Program and documentation. Available from <http://www.cladistics.com>, published by the author, Tucumán, Argentina.
- GOLOBOFF P. A., TORRES A. & ARIAS S. 2017. — Weighted parsimony outperforms other methods of phylogenetic inference under models appropriate for morphology. *Cladistics* 34: 407-437. <http://hdl.handle.net/10539/16138>
- GREGORY W. K. & SIMPSON G. G. 1926. — Cretaceous mammal skulls from Mongolia. *American Museum Novitates* 225: 1-20. <http://hdl.handle.net/2246/3193>
- HERSHKOVITZ P. 1982. — The staggered marsupial lower third incisor (i3). *Geobios, Mémoire spécial* 6: 191-200.

- HERSHKOVITZ P. 1995. — The staggered marsupial third lower incisor: hallmark of Cohort Didelphimorphia, and description of a new genus and species with staggered i3 from the Albian (Lower Cretaceous) of Texas. *Bonner Zoologische Beiträge* 45: 153-169.
- HIEMAE K. & JENKINS F. A. 1969. — The anatomy and internal architecture of the muscles of mastication in *Didelphis marsupialis*. *Postilla* 140: 1-49. <https://www.biodiversitylibrary.org/page/10598728>
- HOROVITZ I. & SANCHEZ-VILLAGRA M. R. 2003. — A morphological analysis of marsupial mammal higher-level phylogenetic relationships. *Cladistics* 19: 181-212. <https://doi.org/10.1111/j.1096-0031.2003.tb00363.x>
- HOROVITZ I., LADEVÈZE S., ARGOT C., MACRINI T. E., MARTIN T., HOOKER J. J., KURZ C., MUIZON C. DE & SANCHEZ-VILLAGRA M. R. 2008. — The anatomy of *Herpetotherium* cf. *fugax* Cope 1873, a metatherian from the Oligocene of North America. *Palaeontographica* 284 (4-6): 109-141. <https://doi.org/10.1127/pala/284/2008/109>
- HOROVITZ I., MARTIN T., BLOCH J., LADEVÈZE S., KURZ C. & SANCHEZ-VILLAGRA M. R. 2009. — Cranial anatomy of the earliest marsupials and the origin of opossums. *PlosOne* 4 (12): 1-9. <https://doi.org/10.1371/journal.pone.0008278>
- KIELAN-JAWOROWSKA Z. 1975a. — Preliminary description of two new eutherian genera from the Late Cretaceous of Mongolia. *Palaeontologia Polonica* 33: 5-16.
- KIELAN-JAWOROWSKA Z. 1975b. — Evolution of the therian mammals in the Late Cretaceous of Asia. Part I. Deltatheridiidae. *Palaeontologia Polonica* 33: 103-132.
- KIELAN-JAWOROWSKA Z. 1977. — Evolution of the therian mammals in the Late Cretaceous of Asia. Part II. Postcranial skeleton in *Kennalestes* and *Asioryctes*. *Palaeontologia Polonica* 37: 65-83.
- KIELAN-JAWOROWSKA Z. 1981. — Evolution of the therian mammals in the Late Cretaceous of Asia. Part IV. Skull structure of *Kennalestes* and *Asioryctes*. Results of the Polish-Mongolian Paleontological Expeditions. Part IX. *Palaeontologia Polonica* 42: 25-78.
- KIELAN-JAWOROWSKA Z. & DASHZEVEG D. 1989. — Eutherian mammals from the Early Cretaceous of Mongolia. *Zoologica Scripta* 18: 347-355.
- KIELAN-JAWOROWSKA Z. & NESSOV L. A. 1990. — On the metatherian nature of the Deltatheroidea, a sister group of the Marsupialia. *Lethaia* 23: 1-10. <https://doi.org/10.1111/j.1502-3931.1990.tb01776.x>
- KIELAN-JAWOROWSKA Z., CIFELLI R. L. & LUO Z.-X. 2004. — *Mammals from the Age of Dinosaurs. Origins, Evolution, and Structure*. Columbia University Press, New York, 630 p. <https://doi.org/10.7312/kiell1918>
- LADEVÈZE S. 2004. — Metatherian petrosals from the late Paleocene of Itaboraí, Brazil, and their phylogenetic implications. *Journal of Vertebrate Paleontology* 24 (1): 202-213. <https://www.jstor.org/stable/4524705>
- LADEVÈZE S. & MUIZON C. DE 2007. — The auditory region of early Paleocene Pucadelphyidae (Mammalia, Metatheria) from Tiupampa, Bolivia, with phylogenetic implications. *Palaeontology* 50 (5): 1123-1153. <https://doi.org/10.1111/j.1475-4983.2007.00703.x>
- LADEVÈZE S. & MUIZON C. DE 2010. — Evidence of early evolution of Australidelphia (Metatheria Mammalia) in South America: phylogenetic relationships of the metatherians from the Late Paleocene of Itaboraí (Brazil) based on teeth and petrosal bones. *Zoological Journal of the Linnean Society* 159 (2): 746-784. <https://doi.org/10.1111/j.1096-3642.2009.00577.x>
- LADEVÈZE S., SELVA C. & MUIZON C. DE 2020. — What are “opossum-like” fossils? The phylogeny of herpetotheriid and peradectids metatherians, based on new features from the petrosal anatomy. *Journal of Systematic Palaeontology* 18: 17, 1463-1479. <https://doi.org/10.1080/14772019.2020.1772387>
- LADEVÈZE S., MUIZON C. DE, BECK R., GERMAIN D. & CÉSPEDES-PAZ R. 2011. — Earliest evidence of mammalian social behaviour in the basal Tertiary of Bolivia. *Nature*. 474: 83-86. <https://doi.org/10.1038/nature09987>
- LOPATIN A. V. & AVERIANOV A. O. 2017. — The stem placental mammal *Prokennalestes* from the Early Cretaceous of Mongolia. *Paleontological Journal* 51 (12): 1293-1374. <https://doi.org/10.1134/S0031030117120048>
- MCKENNA M. C. & BELL S. K. 1997. — *Classification of Mammals above the Species Level*. Columbia University Press, New York, 671 p.
- MARSHALL L. G. 1981. — Review of the Hathlyacyninae, an extinct subfamily of South American “dog-like” marsupials. *Fieldiana Geology*, new series, 7: 1-120. <https://doi.org/10.5962/bhl.title.3520>
- MARSHALL L. G. & KIELAN-JAWOROWSKA Z. 1992. — Relationships of the dog-like marsupials, deltatheroidans and early tribosphenic mammals *Lethaia* 25: 361-374. <https://doi.org/10.1111/j.1502-3931.1992.tb01639.x>
- MARSHALL L. G. & MUIZON C. DE 1984. — Un nouveau Marsupial didelphidé (*Itaboraidelphys camposi* nov. gen. nov. sp.) du Paléocène moyen (Itaboraïen) de Sao José de Itaboraí (Brésil). *Comptes Rendus hebdomadaires des Séances de l'Académie des Sciences*, Paris, sér. II, 299 (18): 1297-1300.
- MARSHALL L. G. & MUIZON C. DE 1988. — The dawn of the age of mammals in South America. *National Geographic Research* 4 (1): 23-55.
- MARSHALL L. G. & MUIZON C. DE 1995. — Part II: The skull, in MUIZON C. DE (ed.), *Pucadelphys andinus* (Marsupialia, Mammalia) from the early Paleocene of Bolivia. Muséum national d'Histoire naturelle, Paris: 21-90 (Mémoires du Muséum national d'Histoire naturelle; 165).
- MATTHEW W. D. 1916. — A marsupial from the Belly River Cretaceous. *Bulletin of the American Museum of Natural History* 35: 477-500.
- MUIZON C. DE 1992. — La fauna de mamíferos de Tiupampa (Paleoceno inferior, Formación Santa Lucía), Bolivia, in SUÁREZ RIGLOS M. (ed.), Fósiles y facies de Bolivia. Vol. I. Vertebrados. *Revista Técnica de Yacimientos Petrolíferos y Fiscales de Bolivia* 12 (3-4): 575-624.
- MUIZON C. DE 1998. — *Mayulestes ferox*, a borhyaenoid (Metatheria, Mammalia) from the early Palaeocene of Bolivia. *Phylogenetic and palaeobiologic implications*. *Geodiversitas* 20: 19-142.
- MUIZON C. DE & ARGOT C. 2003. — Comparative anatomy of the didelphimorph marsupials from the early Palaeocene of Bolivia (*Pucadelphys*, *Andinodelphys*, and *Mayulestes*). Palaeobiologic implications, in JONES M. DICKMAN C. & ARCHER M. (eds), *Predators with Pouches: the Biology of Carnivorous Marsupials*. Surrey Beatty & Sons, Sydney: 42-63.
- MUIZON C. DE & CIFELLI R. L. 2001. — A new basal “didelphoid” (Marsupialia, Mammalia) from the early Paleocene of Tiupampa (Bolivia). *Journal of Vertebrate Paleontology* 21 (1): 87-97. <https://doi.org/brrt8zq>
- MUIZON C. DE & LADEVÈZE S. 2020. — The cranial anatomy of *Andinodelphys cochabambensis*, a stem metatherian from the early Paleocene of the Santa Lucía Formation at Tiupampa (Bolivia). *Geodiversitas* 42 (30): 597-739. <https://doi.org/10.5252/geodiversitas2020v42a30>. <http://geodiversitas.com/42/30>
- MUIZON C. DE, CIFELLI R. L. & CÉSPEDES-PAZ R. 1997. — The origin of the dog-like borhyaenoid marsupials of South America. *Nature* 389: 486-489. <https://doi.org/10.1038/39029>
- MUIZON C. DE, BILLET G., ARGOT C., LADEVÈZE S. & GOUSSARD F. 2015. — *Alcidedorbignya inopinata*, a basal pantodont (Eutheria, Mammalia) from the early Palaeocene of Bolivia: anatomy, phylogeny, and palaeobiology. *Geodiversitas* 37 (4): 397-634. <https://doi.org/10.5252/g2015n4a1>
- MUIZON C. DE, LADEVÈZE S., SELVA C., VIGNAUD R. & GOUSSARD F. 2018. — *Allqokirus australis* (Sparassodonta, Metatheria) from the early Palaeocene of Tiupampa (Bolivia) and the rise of the metatherian carnivorous radiation in South America. *Geodiversitas* 40 (16): 363-459. <https://doi.org/10.5252/geodiversitas2018v40a16>. <http://geodiversitas.com/40/16>

- MURPHY J. L., PUTTICK M. N., O'REILLY J. E., PISANI, D. & DONOGHUE P. C. 2021. — Empirical distributions of homoplasy in morphological data. *Palaeontology* 64 (4): 505-518. <https://doi.org/10.1111/pala.12535>
- NIXON K. 2008. — WinClada, version 1.00. 08. Computer program published by the author, Ithaca, New York, United States.
- NOVACEK M. J. 1986. — The skull of leptictid insectivores and the higher-level classification of eutherian mammals. *Bulletin of the American Museum of Natural History* 183 (1): 1-112. <http://hdl.handle.net/2246/1628>
- OLIVEIRA E. V., ZIMCZ N. & GOIN F. J. 2016. — Taxonomy, affinities, and paleobiology of the tiny metatherian mammal *Minusculodelphis*, from the early Eocene of South America. *The Science of Nature* 103: 6: 1-11. <https://doi.org/10.1007/s00114-015-1331-2>
- RANGEL C. C., CARNEIRO L. M., BERGQVIST L. P., OLIVERIA E. V., GOIN F. J. & BABOT M. J. 2019. — Diversity, affinities, and adaptations of the basal sparassodont *Patene* Simpson, 1935 (Mammalia, Metatheria). *Ameghiniana* 56 (4): 263-289. <https://doi.org/10.5710/AMGH.06.05.2019.3222>
- ROUGIER G. W., WIBLE J. R. & NOVACEK M. J. 1998. — Implications of *Deltatheridium* specimens for early marsupial history. *Nature* 396: 459-463. <https://doi.org/10.1038/24856>
- ROUGIER G. W., WIBLE J. R. & NOVACEK M. J. 2004. — New specimens of *Deltatheroides cretacicus* (Metatheria, Deltatheroidea) from the Late Cretaceous of Mongolia. *Bulletin of the Carnegie Museum of Natural History* 36: 245-266. <https://doi.org/cgbcprc>
- SANCHEZ-VILLAGRA M. R. & SMITH K. K. 1997. — Diversity and evolution of the marsupial mandibular angular process. *Journal of Mammalian Evolution* 4: 119-144. <https://doi.org/10.1023/A:1027318213347>
- SCOTT C. S. & FOX R. C. 2015. — Review of the Stagodontidae (Mammalia, Marsupialia) from the Judithian (Late Cretaceous) Belly River Group of southeastern Alberta, Canada. *Canadian Journal of Earth Sciences* 52: 682-695. <https://doi.org/10.1139/cjes-2014-0170>
- SIGOGNEAU-RUSSELL D., DASHZEVEG D., & RUSSELL D. E. 1992. — Further data on *Prokennalestes* (Mammalia, Eutheria inc. sed.) from the Early Cretaceous of Mongolia. *Zoologica Scripta* 21: 205-209. <https://doi.org/10.1111/j.1463-6409.1992.tb00322.x>
- SINCLAIR W. J. 1906. — Mammalia of the Santa Cruz Beds: Marsupialia. *Reports of the Princeton University expeditions to Patagonia* 4 (3): 333-460.
- SWOFFORD D. L. 2002. — PAUP*: Phylogenetic analysis using parsimony (and other methods), version 4.0b1.0. Sunderland, Massachusetts: Sinauer.
- SZALAY F. S. & TROFIMOV B. A. 1996. — The Mongolian Late Cretaceous *Asiatherium*, and the early phylogeny and paleobiogeography of Metatheria. *Journal of Vertebrate Paleontology* 16 (3): 474-509. <https://www.jstor.org/stable/4523738>
- THEWISSEN J. G. M. 1989. — Mammalian frontal diploic vein and the human foramen caecum. *The Anatomical Record* 223: 242-244. <https://doi.org/10.1002/ar.1092230217>
- TURNBULL W. D. 1970. — Mammalian masticatory musculature. *Fieldiana: Geology* 18 (2): 149-356. <https://doi.org/10.5962/bhl.title.5442>
- WIBLE J. R. 2003. — On the cranial osteology of the short-tailed opossum *Monodelphis brevicaudata* (Marsupialia, Didelphidae). *Annals of the Carnegie Museum* 72 (3): 1-66. <https://www.biodiversitylibrary.org/page/52469617>
- WIBLE J. R. 2008. — On the cranial osteology of the Hispaniolan solenodon, *Solenodon paradoxus*, Brandt, 1833 (Mammalia, Lipotyphla, Solenodontidae). *Annals of the Carnegie Museum* 77 (3): 321-402. <https://doi.org/10.2992/0097-4463-77.3.321>
- WIBLE J. R. 2009. — The ear region of the pen-tailed treeshrew, *Ptilocercus lowii* Gray 1848 (Placentalia, Scandentia, Ptilocercidae). *Journal of Mammalian Evolution* 16 (3): 199-234. <https://doi.org/10.1007/s10914-009-9116-z>
- WIBLE J. R. 2011. — On the treeshrew skull (Mammalia, Placentalia, Scandentia). *Annals of the Carnegie Museum* 79 (3): 149-230. <https://doi.org/10.2992/007.079.0301>
- WIBLE J. R. & ROUGIER G. W. 2000. — Cranial anatomy of *Kryptobaatar dashzevegi* (Mammalia, Multituberculata), and its bearing on the evolution of mammalian characters. *Bulletin of the American Museum of Natural History* 247: 1-124. <https://doi.org/dkppq3>
- WIBLE J. R. & SPAULDING M. 2013. — On the cranial osteology of the African palm civet, *Nandinia binotata* (Gray, 1830) (Mammalia, Carnivora, Feliformia). *Annals of the Carnegie Museum of Natural History* 82 (1): 1-114. <https://doi.org/10.2992/007.082.0101>
- WIBLE J. R., ROUGIER G. W., NOVACEK M. J. & MCKENNA M. C. 2001. — Earliest eutherian ear region: a petrosal of *Prokennalestes* from the Early Cretaceous of Mongolia. *American Museum Novitates* 3322: 1-44. <https://doi.org/ckv3s3>
- WIBLE J. R., NOVACEK M. J. & ROUGIER G. W. 2004. — New data on the skull and dentition in the Mongolian Cretaceous eutherian mammal *Zalambdalestes*. *Bulletin of the American Museum of Natural History* 281: 1-144. <https://doi.org/c4wpk4>
- WIBLE J. R., ROUGIER G. W., NOVACEK M. J. & ASHER R. J. 2009. — The eutherian mammal *Maelestes gobiensis* from the Late Cretaceous of Mongolia and the phylogeny of Cretaceous Eutheria. *Bulletin of the American Museum of Natural History* 327: 1-123. <https://doi.org/10.1206/623.1>
- WILSON G. P., EKDALE E. G., HOGANSON J. W., CALEDE J. J. & VANDER LINDEN A. 2016. — A large carnivorous mammal from the Late Cretaceous and the North American origin of marsupials. *Nature Communications* 7: 13734. <https://doi.org/10.1038/ncomms13734>
- ZIMCZ A. N., FERNÁNDEZ M., BOND M., CHORNOGUBSKY L., ARNAL M., CÁRDENAS M., & FERNICOLA J. C. 2020. — *Archaeogaia macachaae* gen. et sp. nov., one of the oldest Notoungulata Roth, 1903 from the early-middle Paleocene Mealla Formation (Central Andes, Argentina) with insights into the Paleocene-Eocene south American biochronology. *Journal of South American Earth Sciences* 103: 102772. <https://doi.org/10.1016/j.jsames.2020.102772>

Submitted on 1 July 2021;
accepted on 7 October 2021;
published on 30 June 2022.

APPENDICES

APPENDIX 1. — Comment on the scoring of Character 37 in *Marmosopsis*.

Character 37 concerns the relative size of the paracone vs metacone. It includes four states: 0) subequal or slightly larger; 1) slightly smaller; 2) distinctly smaller in volume and height (*c.* 30%); 4) much smaller (*c.* more than 50%). A first observation of the condition in *Marmosopsis* seems to indicate that this taxon could be scored in state 2. However, because this condition is not so clear-cut in the specimens, cast, and photos we have at hand, we have measured the length, width, and height of the paracone and metacone in four cast MNRJ 2478, DGM, 811 and 806), one specimen (MNHN.F.ITB83), and photographs of two specimens (MNRJ 2481 and 2482). The results are given in the Table 5 below.

TABLE 5. — Measurements of the paracone and metacone in *Marmosopsis juradoi*. Abbreviations: **L**, length; **H**, height; **Pa**, paracone; **Me**, metacone; **W**, width.

			L	W	H
MNRJ 2478	M1	Pa	0.41	0.44	0.56
		Me	0.42	0.54	0.78
	M2	Pa	0.34	0.46	0.62
		Me	0.47	0.57	0.84
DGM 811	M3?	Pa	0.52	0.47	0.58e
		Me	0.57	0.59	0.77
DGM 806	M3	Pa	0.47	0.54	0.5e
		Me	0.47	0.57	0.68
ITB 83	M1	Pa	0.44	0.54	0.62
		Me	0.54	0.57	0.86
MNRJ 2481	M1	Pa	0.42	0.45	0.46
		Me	0.58	0.49	0.67
	M2	Pa	0.50	0.58	0.60
		Me	0.64	0.76	0.78
MNRJ 2482	M2	Pa	0.39	0.49	0.43
		Me	0.56	0.59	0.57
	M3	Pa	0.39	0.47	0.54
		Me	0.51	0.64	0.65

As it can be easily calculated, all of the paracone measurements are less than 30% smaller than those of the metacone. Consequently, we have scored *Marmosopsis* in state 1 (paracone slightly smaller than metacone) for character 37.

APPENDIX 2. — Taxon list, references, and specimens.

<i>Aenigmadelphys archeri</i>	Casts of OMNH 20120, 20160, 20531, 20612, 22898, 23321, 23375, 23460, 26169; Cifelli & Johanson (1994);
<i>Alcidedorbignya inopinata</i>	MHNC 1210, 8282, 8287, 8290, 8295, 8298, 8300, 8315, 8359-8363, 8371, 8372, 8373, 8399-8463, 13830-13845;
<i>Allqokirus australis</i>	YPFB pal 6188, 6189, 6190, MHNC 8267; Marshall & Muizon (1988), Muizon (1992);
<i>Alphadon</i> spp.	Eaton (1993);
<i>Alphadon eatoni</i>	Cifelli & Muizon 1998;
<i>Alphadon marshi</i>	Casts of UCMP 47464, 47497, 51385, 51428, 51585, 52502, 52506;
<i>Alphadon wilsoni</i>	Casts of UCMP 46403, 46885, 52767;
<i>Andinodelphys cochabambensis</i>	MHNC 8264, 8306, 8308, 8370, 13847, 13925 13927, 13928 (Five sub-complete skulls and four subcomplete to partial skeletons); Marshall & Muizon (1988), Muizon (1992), Muizon <i>et al.</i> (1997), Muizon & Argot (2003);
<i>Asiatherium reshetovi</i>	cast and original specimen of PIN 3907; Szalay & Trofimov (1996);
<i>Asioryctes nemegtensis</i>	cast of ZPAL MgM-I/56 and I/98; Kielan-Jaworowska (1975a, 1977, 1981, 1984); Horovitz & Sanchez-Villagra (2003); Wible <i>et al.</i> (2004, 2009);
<i>Borhyaena tuberata</i>	YPM-PU 15120, 15701, MACN 2074; Sinclair (1906) Cabrera (1927), Marshall (1981);
<i>Caluromys lanatus</i>	MNHN-ZM-MO-1929-650 , 1929-651 , 1929-652 , 1932-2999 ;
<i>Caluromys philander</i>	MNHN-ZM-MO-1986-140 , 1986-142 , 1986-143 .
<i>Dasyurus hallucatus</i>	MNHN-ZM-MO-1854-99 , 1880-1019; MNHN-ZM-AC-A12425 ;
<i>Dasyurus maculatus</i>	MNHN-ZM-AC-A3295 ; MNHN-ZM-MO-1994-2140 , 1865-32; FMHN 119806, 119805, 119804, 119803;
<i>Dasyurus viverrinus</i>	MNHN-ZM-AC-A2626 , A2627, A3315 ; MNHN-ZM-MO-1882-563 , 1883-1537;
<i>Deltatheridium praetrituberculare</i>	Casts of ZPAL MgM-I/102, ZPAL MgM-I/91, PSS-MAE 132 and 133; Kielan-Jaworowska (1975b); Kielan-Jaworowska & Nessov (1990); Marshall & Kielan-Jaworowska (1992); Rougier <i>et al.</i> (1998);
<i>Deltatheroides cretacicus</i>	Gregory & Simpson (1926); Kielan-Jaworowska (1975b), Rougier <i>et al.</i> (2004);
<i>Didelphis albiventris</i>	MNHN RH 24, 120, 161, MNHN RH uncat.;
<i>Didelphis virginiana</i>	SL uncat.; MNHN-ZM-2007-7 , 2007-12 ;
<i>Didelphis marsupialis</i>	MNHN-ZM-MO-1900-581 , 1900-583 , 1932-3003 ; MNHN-ZM-2007-8 ;
<i>Didelphodon vorax</i>	Cast of USNM 2136, UCMP 52326, 46946, 52342, 51419, 46962, 48189, 48581, 52290, 47304, 53181, 52289. CT data of NDGS 431; UWBM 94500, 94084; SCNHM VMMa 20. Clemens (1966, 1968), Fox & Naylor (1986); Wilson <i>et al.</i> (2016);
<i>Dromiciops gliroides</i>	IEEUACG 2162, IEEUACG 2167; FMNH 22675, FMNH 134556;
<i>Eodelphis browni</i>	Cast of AMNH 14169; Matthew (1916), Fox (1981); Fox & Naylor (2006); Scott & Fox (2015);
<i>Herpetotherium</i> cf. <i>fugax</i>	PIMUZ 2613, MB.Ma 50671, 50672; SMF 2000/168, 2000/169; Gabbert (1998); Horovitz <i>et al.</i> (2008, 2009);
<i>Herpetotherium fugax</i>	AMNH 5254; FMNH P25654, P25653, P15329; Fox (1983), Gabbert (1998);
<i>Incadelphys antiquus</i>	YPFB Pal 6251; MHNC 8270, 13906, 13931, 13932, 13933, 13934, 13935, 13636.
<i>Itaboraidelphys camposi</i>	Casts of DGM 804-M, 814-M, 817-M, 923-M, 926-M; MNRJ 2878-V a and b; Marshall & Muizon (1984);
<i>Kokopellia juddi</i>	OMNH 26361, 34200, 33248, 33243, 27639. Cifelli (1993); Cifelli & Muizon (1997);
<i>Maelestes gobiensis</i>	PPS-MAE-607, Wible <i>et al.</i> (2009);
<i>Marmosa murina</i>	MNHN-ZM-MO-2001-1428 , 2001-1464 , 2001-1966 , 2001-1967 ;
<i>Mayulestes ferox</i>	MHNC 1249 (holotype);
<i>Metachirus nudicaudatus</i>	MNHN RH 16, 81, MNHN RH uncat.; MNHN-ZM-AC-2175 ; MNHN-ZM-2004-316 ; MNHN-ZM-MO-2001-1422 , 1985-1803;
<i>Mimoperadectes houdei</i>	USNM 482355. Horovitz <i>et al.</i> (2009); <i>M. labrus</i> : UM 66144

APPENDIX 2. — Continuation.

<i>Mizquedelphys pilpinensis</i>	YPFB Pal 6196, MHNC 8389, 13917;
<i>Monodelphis brevicaudata</i>	MNHN-ZM-AC-258-M; MNHN-ZM-2004-317 ; MNHN-ZM-MO-1995-3216 , 1967-330. Wible (2003);
<i>Peradectes elegans</i>	Cast of AMNH17383; <i>P. chesteri</i> : cast of UM71663; Crochet 1980;
<i>Peratherium</i> spp.	MNHN.FAU2370, QU8061.R, QU8062.R, QU8063.R, QU8214, QU13371; Crochet 1980;
<i>Prokennalestes trofimovi</i>	PSS-MAE 136; Kielan-Jaworowska & Dashzeveg (1989); Sigogneau-Russell <i>et al.</i> (1992); Wible <i>et al.</i> (2001);
<i>Pucadelphys andinus</i>	MHNC 8265, 8266, 8365, 8376-8395 (all specimens are complete or partial skulls and mandible);
<i>Sipalocyon gracilis</i>	YPM PU 15373, 15154, 15029, AMNH 9254, MACN 691, 692, Sinclair (1906), Cabrera (1927), Marshall (1981);
<i>Sminthopsis crassicaudata</i>	MNHN-ZM-2007-18 , FMNH 60116; FMNH 104788;
<i>Sminthopsis</i> sp.	MNHN-ZO-AC-1919-30, 1892-660;
<i>Szalinia gracilis</i>	MHNC 8350;
<i>Thylamys elegans</i>	MNHN-ZM-MO-1971-1040 , MNHN-ZM-MO-1971-1041 , MNHN-ZM-MO-1971-1042 , MNHN-ZM-MO-1971-1043 .

APPENDIX 3. — List of genus and species names cited in the text with authorship and year.

- Aenigmadelphys* Cifelli & Johanson, 1994
Aenigmadelphys archeri Cifelli & Johanson, 1994
Amphiperatherium Filhol, 1879
Andinodelphys Marshall & Muizon, 1988
Andinodelphys cochabambensis Marshall & Muizon, 1988
Asiatherium Trofimov & Szalay, 1994
Asiatherium reshetovi Trofimov & Szalay, 1994
Asioryctes Kielan-Jaworowska 1975
Asioryctes nemegtensis Kielan-Jaworowska 1975
Borhyaena Ameghino, 1887
Borhyaena tuberata Ameghino, 1887
Callistoe Babot, Powell & Muizon, 2002
Caluromys Allen, 1900
Caluromys lanatus Olfers, 1818
Caluromys philander Linnaeus, 1758
Dasyurus Geoffroy Saint-Hilaire 1796
Dasyurus hallucatus Gould, 1842
Dasyurus maculatus (Kerr 1792)
Dasyurus viverrinus (Shaw, 1800)
Deltatheridium Gregory & Simpson, 1926
Deltatheridium pretrituberculare Gregory & Simpson, 1926
Deltatheroides Gregory and Simpson, 1926
Deltatheroides cretacicus Gregory & Simpson, 1926
Didelphis Linnaeus, 1758
Didelphis albiventris Lund, 1840
Didelphis marsupialis Linnaeus, 1753
Didelphis virginiana Kerr, 1792
Didelphodon Marsh 1899
Didelphodon vorax Marsh 1899
Dromiciops Thomas, 1894
Dromiciops gliroides Thomas, 1894
Eodelphis Matthew, 1916
Eodelphis browni Matthew, 1916
Herpetotherium Cope, 1873
Herpetotherium fugax Cope, 1873
Incadelphys antiquus Marshall & Muizon, 1988
Itaboraidelphys Marshall & Muizon, 1984
Itaboraidelphys camposi Marshall & Muizon, 1984
Kokopellia Cifelli, 1993
Kokopellia juddi Cifelli, 1993
Kryptobaatar Kielan-Jaworowska, 1969
Maelestes Wible, Rougier, Novacek, & Asher, 2007
Maelestes gobiensis Wible, Rougier, Novacek & Asher, 2007
Marmosa Gray, 1821
Marmosa murina Linnaeus, 1758
Marmosops Matschie, 1916
Marmosopsis, Paula Couto, 1962
Marmosopsis juradoi Paula Couto, 1962
Mayulestes Muizon, 1994
Mayulestes ferox Muizon, 1994
Metachirus Burmeister, 1854
Metachirus nudicaudatus Geoffroy Saint-Hilaire, 1803
Mimoperadectes Bown & Rose, 1979
Mimoperadectes houdei Horovitz, Martin, Bloch, Ladevèze, Kurz & Sánchez-Villagra, 2009
Mimoperadectes labrus Bown & Rose, 1979
Mizquedelphys Marshall & Muizon, 1988
Mizquedelphys pilpinensis Marshall & Muizon, 1988
Monodelphis Burnett, 1830
Monodelphis brevicaudata (Erxleben, 1777)
Patene Simpson, 1935
Patene coluapiensis Simpson, 1935
Patene simpsoni Paula Couto, 1952a
Peratherium Aymard, 1850
Prokennalestes Kielan-Jaworowska & Dashzeveg, 1989
Prokennalestes trofimovi Kielan-Jaworowska & Dashzeveg, 1989
Pucadelphys Marshall & Muizon, 1988
Pucadelphys andinus Marshall & Muizon, 1988
Sipalocyon Ameghino, 1887
Sipalocyon gracilis Ameghino, 1887
Sminthopsis Thomas, 1887
Sminthopsis crassicaudata (Gould, 1844)
Szalinia Muizon & Cifelli, 2001
Szalinia gracilis Muizon & Cifelli, 2001
Thylamys Gray, 1843
Thylamys elegans Waterhouse, 1839
Wynyardia bassiana Spencer, 1901
Zalambdalestes Gregory & Simpson, 1926
Zalambdalestes lechei Gregory & Simpson, 1926
Zhangheotherium Hu, Wang, Luo & Li, 1997